E-137

July 29, 1980

Proposal To Search For Low Mass, Metastable, Neutral Particles at SLAC

Submitted by

A. Abashian, J. D. Bjorken, L. W. Mo*,

W. R. Nelson and Y. S. Tsai

Fermilab - SLAC - VPI and State University

July, 1980

*Correspondent

Table of Contents

Abstract

We propose to conduct a beam dump experiment at SLAC to search for the low mass (1 - 200 MeV), metastable, neutral particles made by a highly collimated production mechanism. A fine-grained shower detector is proposed to be installed at a location east of the Beam-dump A to look for their electromagnetic decays.

I. Introduction

The existing list of elementary particles, while large and rather well-organized, may not be complete. It is without question important to search for unexpected particles in as many ways as practical. We propose to carry out a search for neutral, penetrating unstable particles X, taking advantage of features unique to SLAC. The method, a beam-dump experiment, bears similarity to the "Black Hole" SLAC experiment[1] E - 56. However, we propose to only search for the decay-products of X, not its interactions, and should extend the sensitivity of the previous experiment by considerably more than a factor 100.

The best candidates for detectable X-particles seem to be neutral spinless axion-like objects, or neutral spin-1/2 neutrino-like objects with small mass, anywhere from the sub-MeV range to the sub-GeV range. A special feature peculiar to SLAC is that there exist production mechanisms that maintain very good collimation of the beam of such X-particles emergent from the dump. This allows a long decay region without unacceptable loss of particles from angular divergence. A second special feature is the extremely high intensity of e^-, e^+ and γ in the SLAC dump. The combination of these features makes SLAC superior to proton machines by several orders of magnitude in searching for certain classes of X particles. The detailed definition of these classes will be explicated in Section II. However, it must be kept in mind that those theoretical considerations should be viewed as only the roughest guideline as to the sensitivity of the search. Were a positive effect to be seen, it is quite likely that it would not correspond to the scenarios our poor imaginations are able to construct. (In this regard, one may remember that the 1970 SLAC beam dump experiment was originally[1] discussed

in terms of photoproduction of τ-like leptons, with detection of the associated neutrinos, while its greatest usefulness was eventually in axion searches.[2])

The basic layout of the proposed experiment is shown in Fig. 1. The primary SLAC electron beam, of highest energy and intensity possible, is transported to a standard $H_2O/A\ell$ high power dump. This is followed by a shield sufficiently thick to range out the highest energy muons. This in turn is followed by a long (50-200 m) decay region, beyond which is the detector, of area $\sim$5-10 m^2. This detector accurately measures the energy and direction of electromagnetic showers induced by decay products ($e^{\pm}$ or γ) of the X. Several possibilities for the location and configuration of this experiment have been studied, and are described in Section III. Our preferred choice is to use Beam-dump East in the berm behind end station A (as in E-56) and locate the detector on a hilltop near the site boundary, northeast of PEP interaction region 2. This location is $\sim$430 m downstream of the dump, and views $\sim$200 m of decay space.

The detector is in existence at Fermilab. There it was used in experiment E-253 at Fermilab[3], which successfully observed the process $\nu_\mu + e^- \rightarrow \nu_\mu + e^-$. Both in that experiment and in this proposed experiment, detection of pure electromagnetic showers, along with accurate measurement of their angles and energies, are the crucial requirements. The properties of the detector and its proposed reconfiguration are discussed in Section IV.

Other than the large amount of beam, the requirements on SLAC are minimal. We require site preparation and housing for the experiment, a modest amount of power and electronics from the pool, a timing signal from the linac, and a steering magnet in Beam-dump East to direct the primary electrons upward by $\sim$15 mr before entering the dump.

Our major request is a large amount of beam (30 coulombs of electrons). This is a difficult point, especially given the competing demands on the Laboratory and given that the probable outcome of the experiment is nothing at all. However, upon comparing the cost of this experiment with the amount of effort which goes into relatively predictable, programmatic studies, we believe that the expenditure is not inordinate, and that the very high risk is justifiable.

II. Physics Goals

We shall assume a geometry compatible with Fig. 1, where the distance from dump to detector is ~100-500 m, and where the cross-sectional area of the detector is ~5-10 m^2. The solid angle subtended is very small, suggesting that we focus attention on possible low mass (1-200 MeV), metastable, neutral particles made by a highly collimated production mechanism. Three different production mechanisms (Fig. 2), quite unique to SLAC, come to mind:

(1) Production of boson X via the Primakoff process, followed by its decay into two photons.

(2) Production of a boson X via Bremsstrahlung from an electron.

(3) Production of a lepton (or boson) via annihilation of a positron (produced in the electron-initiated cascade) with an atomic electron.

The most difficult question concerning this experiment has to do with credibility: Is it reasonable that particles with properties appropriate for detection in this experiment really exist? Would such particles have been found in other experiments? Would existence of such particles conflict with the currently accepted theoretical descriptions of strong and electroweak interactions, or could they be incorporated into such a framework? The answers to these questions are not very encouraging. Nevertheless, it is possible to construct some examples of phenomena for which this experiment would be sensitive.

The processes (1) and (2) are most usefully discussed in the context of axion-production. Searches for the "classical" axion have been negative-almost decisively so.[2,4,5] Furthermore, this proposed experiment is not an improvement, because it is more advantageous to search for interaction of a "classical" axion with hadrons than to search for its decay. Nevertheless, it is possible that other kinds of axions, in particular axions which do not

couple to light quarks or electrons, might exist. Such an axion field would be the divergence of some axial current built out of other degrees of freedom (techniquarks?).[6,7] If this is the case, we may expect such a particle to decay into two photons, with a width which can be scaled from π° decay. Specifically

$$\frac{\Gamma_{X\to\gamma\gamma}}{\Gamma_{\pi^\circ\to\gamma\gamma}} = K \left(\frac{m_X}{m_{\pi^\circ}}\right)^3 \left(\frac{F_\pi}{F_X}\right)^2$$

where K is a group-theoretical factor of order unity ($K = 2\Sigma_i Q_i^2 T_{3i}^{(axial)}$, where the sum goes over fermion species which couple to the axial-current appropriate to the axion), and where F_X is the analogue of the pion decay constant. (In technicolor models,[6,7] the parameter F_X is typically 100-300 GeV.) Hereafter we shall set K = 1 in making estimates.

Production of an axion via the Primakoff mechanism has a very strong kinematic similarity to production of an electron-positron pair. The Primakoff cross-section is (per nucleon)

$$\sigma_X = \frac{8\pi\alpha}{A}\frac{\Gamma_X}{m_X^3}\int_{t_{min}} dt\frac{(t-t_{min})}{t^2}\ G(t)$$

while the pair-production cross-section is (per nucleon)

$$\sigma_{pair} \simeq \frac{16}{9}\frac{\alpha^3}{Am_e^2}\int dt\frac{(t-t_{min})}{t^2}\ G(t)$$

The ratio of these cross-sections therefore gives, approximately,[8] the probability per photon in the dump that it makes an axion before being converted. The flux of axions is thus closely proportional to the track

length of photons in the dump. Furthermore their angular distribution is essentially the same as that of the photons, because of the very small values of the typical momentum transfers $\sqrt{t}$ in the Primakoff process.

Calculation of photon track length (radiation length per GeV) dN_γ/dE in an Aℓ dump has been carried out using the EGS Monte Carlo program,[9] and the result is shown in Fig. 3 for incident energies of 15 GeV and 30 GeV. The angular distributions at various photon energies have also been computed (Fig. 4). For the anticipated geometry, with an approximately circular detector of radius ~1.5 m located 430 m from the dump, the detection efficienty $\varepsilon(E)$ of the detector (making the crude assumption that decay products of axions aimed at the detector are observed, while axions which would miss the detector are not observed) is shown in Fig. 5.

Armed with all these details, the expected differential flux through the detector of axions of energy E per incident electron of energy E_0 is given by

$$\frac{dN_X}{dE} \simeq \frac{7}{9} \cdot \frac{9\pi}{2\alpha^2} \cdot \frac{m_e^2 \Gamma_X}{m_X^3} \cdot \varepsilon(E) \frac{dN_\gamma}{dE}$$

To estimate the number of detected axions, we must know the decay probability. Assuming the only open decay channel is $X \to \gamma\gamma$. the decay length λ_X is

$$\lambda_X = \left[\frac{E_X}{m_X}\right] \frac{c\tau_{\pi^0}}{K} \left[\frac{m_\pi}{m_X}\right]^3 \left[\frac{F_X}{F_\pi}\right]^2$$

and the decay probability is

$$P = e^{-L/\lambda_X} \left[e^{\ell/\lambda_X} - 1\right] \simeq \ell/\lambda_X \qquad \text{for } L << \lambda_X$$

where

ℓ = length of decay region ($\sim$200 m)

L = distance from dump to detector ($\sim$430 m).

We may now put together these numbers and estimate the number of detected axions per coulomb of incident electrons.

It turns out in the range of interest the decay length is long compared to 500 m. The net result for the axion production is simple:

$$\text{Detected axions per coulomb of } e^- \simeq \begin{cases} 2.6 \times 10^{-4} \left(\frac{m_X}{F_X}\right)^4 & E_o = 15 \text{ GeV} \\ 5.6 \times 10^{-4} \left(\frac{m_X}{F_X}\right)^4 & E_0 = 30 \text{ GeV} \end{cases}$$

The result is shown in Fig. 6 as a contour plot of detected axions/coulomb versus axion mass m_X and the fundamental decay parameter F_X. Assuming that 0.3 detected events/coulomb is an observable signal, the available open window in F_X-m space is modest, but still significant. This is especially the case because values of F_X in the range 100 GeV - 10 TeV are interesting from the point of view of technicolor models. We also see that the improvement over the 1970 SLAC dump experiment is very significant.

The second option supposes an axion with significant coupling to e^+e^-, but no significant coupling to $\gamma\gamma$ or quarks. Then the axion may be produced via bremsstrahlung from electron lines. This was calculated by Donnelly et al.,[2] who, assuming production by first-generation electrons only, show that the number of produced axions per incident electron is

$$E \frac{dN_X}{dE} \simeq \frac{1}{6\alpha} \left(\frac{g^2}{4\pi}\right)$$

where g is the axion-electron pseudoscalar coupling constant. The angular distribution of electrons in the dump is considerably broader than the photon angular distribution; hence the efficiency factor will be somewhat lower at lower energies (c.f. Fig. 5). (Because the radiated axion tends to take most of the parent electron's energy, it should not be too bad an approximation, and in any case a conservative one, to equate the angular distribution of axions of a given energy with that of the electrons of the same energy.) Actually the procedure used seriously underestimates the yield. We have not yet completed the recalculation, but we expect an enhancement by a factor $\sim$3-10.

The decay width of the axion (assuming the e^+e^- channel is dominant), is given by

$$\Gamma_X = \frac{m_X}{2}\left(\frac{g^2}{4\pi}\right)$$

From this, we may repeat the previous analysis, now in $(g^2/4\pi)$ - mass space. The result is shown in Fig. 7. We see that the precious dump experiment had considerably less sensitivity, and that there is a large improvement in the range of parameters accessible.

We note that if we take the nominal value of $g^2/4\pi$ suggested by theory

$$\frac{g^2}{4\pi} \simeq \frac{1}{4\pi}\left(\frac{m_e}{F_X}\right)^2$$

and set it equal to the value 3×10^{-17} for which the experiment is sensitive, this implies that $F_X \sim 25$ TeV!! This is a range of F_X which is compatible with order-of-magnitude estimates associated with extended technicolor.[6,7] The window of observability may be small for this

particular process, but the sensitivity is exquisite.

We finally turn to the third possibility, namely production of leptons via positron-electron annihilation. The luminosity is very high (10^{10} nb^{-1}/day), but unfortunately the observability is rather poor. At least two processes seem possible in principle:

$$e^+e^- \to L^o + \nu \qquad (a)$$

$$e^+e^- \to L^o + \bar{L}^o \qquad (b)$$

The first process (a) has the virtue that it provides a built-in decay mechanism. However, electroweak theory does not provide any rationale for existence of such a process. We take a not-very credible hypothesis that process (a) is not mediated by gauge-quanta, but something else (Higgs?). It will have two basic parameters, the coupling-strength G and lepton mass m_L. The second process is credible, provided L^o is a (massive) neutrino associated with a 4th-generation charged lepton L^+. In that case, annihilation via Z^o can be calculated. However, there is no specified mechanism for decay.

Let us now look at the first option (a). We take the production cross-section of typical weak form, but including an appropriate threshold factor

$$\sigma \sim \frac{G^2 S}{4\pi} \left(1 - \frac{m^2}{S}\right)^2$$

Here G is merely a phenomenological parameter which characterizes the coupling-strength, not to be confused with the Fermi-constant G_F. This production cross-section must then be convoluted <u>with the positron flux in the dump</u>.

The EGS program[9] provides us with the track length as function of energy. This can be convoluted against the production cross-section to obtain the differential flux of leptons. Integration over the energy distribution of electrons then gives the yield of leptons.

The decay probability (assuming $L^0 \to e^+e^-\nu$ is the only open channel) may be scaled from muon decay:

$$\frac{\Gamma_L}{\Gamma_\mu} \simeq \left(\frac{G}{G_F}\right)^2 \left(\frac{m_L}{m_\mu}\right)^5$$

Again, from the width the decay-probability can be computed. With all this information, the number of "observed" leptons as function of G and M can be computed. The result (Fig. 8) is that the rate is very sensitive to the mass, to G, and to incident energy E_0. For $m_L \sim m_\mu$, and 0.3 events/coulomb as signal we need, at E_0 = 30 GeV, $G/G_F \gtrsim 1$. This is a relatively large coupling, but not, perhaps, out of the question.

Finally, for case (b), we may consider the production of L^0-$\bar{L}^0$ pairs which are members of a weak doublet. This proceeds by annihilation via Z_0. The Weinberg-Salam effective Lagragian is

$$\mathcal{L} \simeq \frac{G_F}{2\sqrt{2}} \left[\bar{e}\gamma_\mu e(1-4\sin^2\theta_W) + \bar{e}\gamma_\mu\gamma_5 e\right] \bar{L}\gamma^\mu(1-\gamma_5)L$$

Taking $\sin^2\theta_W = 1/4$ for a simple estimate gives

$$\sigma \simeq \frac{G_F^2 S}{48\pi}\left(1 - \frac{m^2}{S}\right)\sqrt{1 - \frac{4m^2}{S}}$$

The same procedure as before may be followed, leading to the number of detected leptons (assuming 100% efficiency) as function of mass and life-time (Fig. 9). Also shown there is the region excluded by the previous

SLAC dump experiment.

We conclude that there is, for all these options, a reasonable, but not overwhelmingly large, region of parameter-space which can be explored, and which is quite unique to this technique.

III. Design Considerations

A. Configuration and Location:

We have considered several possible configurations and locations for this experiment. They are shown in Fig. 10, and discussed in turn below:

(1) This, our preferred choice, is the configuration already described. The primary beam is transported to beam-dump east, bent upward by ∿14 mr (by a new bending magnet) just before entering the dump. There exists ∿230 m of earth shielding followed by ∿200 m of decay path. The detector is located near the site boundary on a hill northeast of PEP interaction region 2. Without the bending magnet, the decay region is reduced to a length of ∿145 m (c.f. Fig. 11).

(2) A new dump, followed by an iron shield of length ∿20 m, is installed in the A switchyard downstream of the final bend and upstream of the stub leading to SPEAR. The rear wall of End Station A is removed, and the detector is placed in front of Beam Dump East. This gives a dump-to-detector distance of ∿220 m and a decay volume of length ∿140 m. If the detector is put in End Station A, the length of the decay region is reduced to ∿70 m.

Advantages of this layout are that it does not involve a remote location with its possible logistics problems and that the dump-detector distance is halved, thus improving the solid-angle greatly. Possible disadvantages are the complexity of the dump configuration, making the interpretation of a candidate signal much more problematic. Also, any concurrent physics program in End Station A is precluded. There may also be a limitation on the maximum incident energy, either from fiscal constraints or from lack of space in the tunnel for adequate shielding.

(3) A new dump and iron shielding is provided in the C switchyard, and the length of the research yard is used as the decay region. This configuration is, in principle, probably the optimal one if the detector remains in the research yard and does not take to the hills, However, it appears costly and very disruptive to the bubble-chamber program.

(4) The beam is transported to and dumped in the existing LASS dump upstream of End Station B. The exiting beam line, which emerges at an upward angle of 1.0°, penetrates the berm behind the research yard and briefly re-emerges above grade near PEP region 4. In that region there exists ∿45 m of decay space. The detector location is east of the PEP access road, and north of the PEP-4 experimental hall. Were it possible to deflect the primary electron beam upward another 0.5° before being dumped, the decay region could be increased to ∿125 m.

The advantage to this option lies in the possibility of parasitic running with the LASS program. A disadvantage is that the existing dump does not handle the full beam power. We estimate that in 1500 hours of LASS running we would accumulate ∿40 coulombs of electrons into the dump. Another disadvantage is the large dump-to-detector distance and small decay volume.

The basic parameters for these options are summarized in the following table.

Table

			Distance from Dump (m)	Length of Decay Space (m)
I.	Beam-dump East Detector on hill near PEP-2	steered beam	430	205
		(unsteered beam)	(365)	(145)
II.	Dump in A switchyard	Detector in front of beam dump east	220	140
		(Detector at rear of End Station A)	(150)	(70)
III.	Dump in C switch-yard Detector at rear of research yard		240	215
IV.	LASS dump	unsteered beam	455	45
	Detector on hill near PEP-4	(steered beam)	(490)	(125)

A figure-of-merit for each of these designs (in the context of the physics goals discussed in Section II) is the product of detection efficiency (as defined in the simple-minded way in the previous section) and the length of the decay space. (We again assume a circular detector of radius 1.5 m.) This is plotted in Fig. 12. We see that because the efficiency of the distant detector is always $\gtrsim$ 40% for photons and $\gtrsim$20% for electrons and positrons, there is not a large advantage in the designs with a shorter dump-to-detector distance. However, in studying Fig. 12, one should keep in mind that many of the events are at relatively low energy, where the relative-efficiency effects are the largest. It seems clear that Option IV is inferior, and Option III sufficiently close to II that the additional practical difficulties of III argue in favor of II.

The main choice, therefore, lies between Options I and II. While many pros and cons may be written down, the relative unambiguity of interpretation of a positive signal for configuration I seems to us to be the overriding consideration.

B. Backgrounds

The backgrounds in location I may be divided into 4 categories.

(i) Cosmic rays: The cosmic ray background is much less serious than that in the Fermilab experiment E-253, which recorded events over a live-time of $\sim$200 hours. The low SLAC duty factor makes the live time of this experiment only a few hours. (In fact the cosmic rays will be useful to monitor the apparatus.)

(ii) Skyshine: Skyshine (capture γ-rays from low-energy neutrons) is out of time and should be able to be easily shielded.

(iii) Muon (or hadron) bursts from the top of the berm: If the experiment is run concurrently with a program in End Station A, muons

(or hadrons) from the target point may scrape the top of the berm, with the electromagnetic products of an interaction seen in the detector. A very crude estimate gives $\lesssim 1$ detected shower per coulomb of electrons. However a larger number would be no problem, because the top of the berm subtends an angle of $\sim$20-30 mrad, which is much larger than the angular resolution of the detector. It is furthermore distinguishable as a line source, and can of course be eliminated entirely.

(iv) Production of neutrino interactions in the surface of the berm viewed by the detector: These are crudely estimated to be <1 event/coulomb, and are distinguished by their broad angular distribution.

(v) Secondary interactions of the punch-through hadrons: The background arising from the interactions of the punch-through hadrons with the air ($\sim$20 g) in the decay region is estimated to be negligible. More careful investigation is still underway.

IV. Experimental Apparatus

The detector we plan to use in this proposed SLAC experiment is the one employed at Fermilab for the measurement of the $\nu_\mu + e^- \rightarrow \nu_\mu + e^-$ reaction. Its arrangement is shown schematically in Fig. 13. Basically, it is a fine-grained calorimeter made of 49 identical modules. Each module consists of one 1 r.l. thick aluminum plate, one multi-wire proportional chamber (MWPC) with cathode plane delay-line readouts, and one layer of plastic scintillators. Their dimensions are 1 m x 1 m each in cross sectional area.

At SLAC, we will stack the detector into a 2 m (vertical) x 3 m (horizontal) x 8 r.l. (depth) assembly. Immediately in front and behind this calorimeter assembly, we will install two scintillation hodoscopes. In case the muon-decay mode were observed, we would like then to consider the possibility of installing a muon detector behind the calorimeter. This muon detector will consist of a magnetized iron shield, 2-1/2 m x 3 m in area and 1 m in depth, and a set of drift wire chambers. We have 12 drift wire planes 2 m x 2 m in size. Initially, this muon detector will not be installed.

In the following sections, we will briefly explain the mechanics of the experimental apparatus.

(1) The MWPC

The schematic of the MWPC is shown in Fig. 14. The anode wires in each chamber are electrically connected together. Their common signal is fed into an ADC to measure the energy deposition and also used to form the experimental trigger. Delay-lines on the two cathode planes of one MWPC are arranged along orthogonal directions to measure both x- and y- positions of traversing particles in terms of time intervals. The technical details are described in Appendix 1.

This delay-line configuration offers a number of advantages other than being economic. For electromagnetic showers, there are too many particles involved in each chamber. It would be a difficult task in trying to digitize every one of them. By capacitive action, this group of particles will induce a localized cluster of charges on the cathode planes. Afterwards, the induced pulse train will propagate along the long transmission line to the tap points, then be fed into the time-to-digital converters (TDC's) to measure the edges of the electromagnetic shower. Shower centroid is assumed to be the midpoint of the two edges. A least-square-fitted straight-line with the first 5 r.l. of the detector is used to determine the angle of the electromagnetic shower. Fig. 15 illustrates the procedure and Fig. 16 gives the test results at Cornell University on the angular resolution.

Fig. 17 shows a candidate of $\nu_\mu e^-$ elastic scattering obtained at Fermilab. It is clear from this picture that the angular measurement of the shower should be done only with the first 5 r.l. If more radiation lengths are included, the angular resolution will deteriorate because of the large spatial fluctuations caused by the absorption of the low energy components of the shower.

Using this technique, an angular resolution of $\sim\pm5$ mr was achieved and it was good enough to do the $\nu_\mu e^-$ scattering experiment at Fermilab. The existing equipment is certainly adequate for the proposed experiment at SLAC because its requirement is very similar to that of $\nu_\mu e^-$ elastic scattering.

In connection with a new neutrino experiment proposed to Fermilab, we try to further improve the angular resolution by a factor of 5 to the value of $\sim\pm1$ mr. The technique lies in the improvement of the TDC electronics

which will be discussed in the next section.

(2) The CCD Digitizer

We have successfully developed a new type of TDC's using charge-coupled devices (CCD's) to improve our detector resolution. These CCD digitizers will be used on the cathode plane delay-lines. The principle of this device is illustrated in Fig. 18. The CCD is continuously clocked at 50 MHz. The incoming pulse from a given cathode-plane tap is thus quantized into 20 nsec intervals. Charges contained in each interval will be loaded into successive CCD buckets. For each clock pulse, the charges in each bucket will shift one bucket position. When it reaches the end, a fast ADC will start to act, digitizing the charges stored in each bucket successively. By the mean time, a scanner will keep track of the CCD bucket number. In essence, the CCD digitizer works like a superscope because it retains the complete information of the profiles of the pulses on the delay-line. The charge information will provide measurements of energy depositions. The CCD bucket numbers will yield the track position information. Using this technique the track positions can be measured more accurately. Since the pulse profile (or the charge distribution along the transverse direction) is known, we can weigh the position measurements by the corresponding charges to obtain the centroid positions properly. Unlike the presently used method of measuring only the shower edges, the effects due to noise and signal dispersion, etc., should become negligible for the case of CCD's. We anticipate that the angular resolution can be improved to $\sim \pm 1$ mr. Also, we do not need tilted wire planes to resolve the combinatorial ambiguities. The absolute position of a particle (or the centroid of an electromagnetic shower) is given simply by the propagation time along the delay-line.

Another important aspect of the CCD digitizer is that it enables us to measure both the energy and the direction of each individual particle of a multiple-track event, provided that the tracks do not overlap. This is achieved by following the track and adding up the energy depositions. This capability should prove to be a breakthrough in calorimetry. It is the only way we know of which can measure both directions and energies of individual particles by a non-magnetic calorimeter.

We are currently in the process of converting the existing E-253 electronics into CCD digitizers. The task involves replacing all the amplifiers and TDC's on the 49 MWPC's. Altogether, there are 490 channels of CCD digitizers. It is anticipated that the electronics can be finished this year. We will make a test run at either Fermilab or SLAC to learn the performances of these devices. We will measure the energy and the angular resolutions for various particles and to develop the necessary softwares for the proposed experiment.

Our proposed experiment at SLAC does not depend on the CCD digitizers. But if time permits, we will use them to improve the quality of the experiment. Before making the switch, tests and calibrations on these new devices have to be done first.

(3) The Scintillation Counter

In the calorimeter, there is one layer of plastic scintillation counter in every detector module. We use them to measure the energy deposition, which will double check that measured by the MWPC's. Also, they are used to form the experimental triggers.

(4) The Trigger

We will analogly add up the MWPC anode signals from the first 6 r.l. and then make energy discriminations to pick up the triggers corresponding

mostly to electromagnetic showers. For the plastic scintillation counters, we will discriminate the signals first and then make a logical AND. The master trigger is the coincidence between the logical output of the MWPC's and that of the plastic scintillation counters. The use of the plastic scintillation counters improves the time resolution.

The muon trigger is also provided by the plastic scintillation counters in the calorimeter. The signals go through X10 gain amplifiers first, and then form the trigger by the majority logic. This trigger is useful in timing the counters, checking equipment with cosmic rays, etc.

V. Manpower and Resources

In addition to the proponents of this proposal, we plan to add one to two research associates from VPI. Probably we can add some graduate students. Also, we are inviting new collaborators who are interested in this proposed experiment at SLAC

On the technical side, we are properly equipped to handle the experiment. T.A. Nunamaker has been in charge of the equipment construction, maintenance, and development. For years, we have been using the skilled personnel and good shop facilities of the Nanometric System Inc. for equipment manufacturing and maintenance.

In this collaboration, the Fermilab and SLAC phycists are supported by the Department of Energy contracts; physicists from VPI, by NSF and the University.

VI. The Request

For this proposed search experiment at SLAC, we request the Laboratory to provide us the following items:

(1) An integrated charge of 30 coulombs of accelerated electrons in the energy range of ∿20 - 30 GeV, but not lower than 15 GeV.

(2) An adequate housing (∿600 square ft) and electric power for the detector and associated counting electronics. The equipment is listed in Appendix 2.

(3) Beam monitoring equipment and timing signal from the accelerator.

(4) Fast electronics from HEEP. They are all standard commercial items which includes power supplies, discriminators, logic units, ADC's, etc. The detailed list is included in this proposal as Appendix 3.

(5) 100 hours of computer time at SLAC computer center for Monte Carlo calculations, data checking, etc.

(6) Mechanical structure to stack the detectors.

(7) A period of ∿ 3 weeks for calibration and testing with a weak beam of electrons and/or hadrons in the test beam area.

(8) A steering magnet which can bend the primary electrons upward by ∿15 mr before entering the Beam-dump East.

References

1. SLAC Experimental Proposal E-56, by D. Dorfan, D. Fryberger, J.M Gaillard, D. Kreinick, A. Mann, A. Rothenberg, M. Schwartz, and T. Zipf. For the experimental results see A. F. Rothenberg, SLAC Report No. 147, 1972 (unpublished).
2. T. W. Donnelley, et al., Phys. Rev. D18, 1607 (1978).
3. R. H. Heisterbert, et al., Phys. Rev. Lett. 44, 635 (1980).
4. S. Weinberg, Phys. Rev. Lett. 40, 223 (1978).
5. F.Wilczek, Phys. Rev. Lett. 40, 279 (1978).
6. S. Dimopoulos "Technicolored Signatures" Stanford University, Preprint 79-0962 (1979).
7. E. Eichten and K. Lane, Phys. Lett. 90B, 125 (1980).
8. The integration with respect to the target form factor G(t) depends upon t_{min} which is $m_x^4/(2k)^2$ for X production and $(2m_e)^4/(2k)^2$ for electron pair production. We are interested in the kinematical region k > 2 GeV and $k/M_x > 300$. In the X production the integration yields

$$\chi_x = Z^2 [2 \ell n(k/M_x) - 1]$$

corresponding to the limit of point nucleus and no atomic screening, whereas

$$\chi_{pair} = Z^2 [2 \ell n (111 Z^{-1/3}) - 1] + Z[2 \ell n(773 Z^{-2/3}) - 1]$$

corresponding to the limit of complete screening in the Fermi-Thomas model. (See K. J. Kim and Y. S. Tsai, Phys. Rev. D8, 3109 (1973)). We approximate χ_x by χ_{pair}, which in general underestimates the yield of X.

9. W. R. Nelson SLAC Report 210 (1978), "EGS Code System: Computer Programs for the Monte Carlo Simulation of Electromagnetic Cascade Showers".

Figure Captions

Fig. 1 Schematic layout of the proposed experiment.

Fig. 2(a) Photoproduction of axion coupled to $\gamma\gamma$

(b) Electroproduction of axion coupled to e^+e^-.

(c) Single lepton production by positron annihilation.

(d) Lepton pair production by positron annihilation.

Fig. 3 Photon track length vs photon energy E for incident electron energy (a) E_0 = 15 GeV, (b) E_0 = 30 GeV

Fig. 4 $P_\perp$ or angular distributionof photons at various energies for incident electron energy E_0 = 15 and 30 GeV. The vertical scale is arbitrary.

Fig. 5 Detection efficiency vs photon energy E for incident electron energy E_0 = 15 or GeV. The detector is assumed to be circular of radius 1.5 m and located 430 in from the electron beam dump.

Fig. 6 Contour plotof detected axions/coulomb in the F_x-m plane. The axions are coupled to $\gamma\gamma$ and the incident electron energy is (a) E_0 = 15 GeV, (b) E_0 = 30 GeV.

Fig. 7 Contour plot of detected axions/coulomb in the $(g^2/4\pi)$-m plane. The axions are coupled to e^+e^-. The calculation is independent of incident electron energy E_0. It is conservative by a factor of $\sim$ 5 to 10.

Fig. 8 Contour plot of detected events/coulomb for the process $e^+e^- \rightarrow L^0\nu$ in the (G/G_F) - m plane. The incident electron energy is (a) E_0 = 15 GeV, (b) E_0 = 30 GeV.

Fig. 9. Contour plot of detected events/coulomb for the process $e^+e^- \to L^oL^o$ in the τ-m plane. The incident electron energy is (a) E_o = 15 GeV, (b) E_o = 30 GeV.

Fig. 10 Schematic of several possible configurations and locations for this proposed experiment at SLAC.

Fig. 11 Schematic of the preferred arrangement for this proposed experiment at SLAC.

Fig. 12 Figure-of-merit (product of detection efficiency with length of decay region) vs photon energy for various options of experimental configurations for axions coupled to (a) $\gamma\gamma$, (b) e^+/e^-. The options denoted with or without parenthesis correspond to that given in the table of P. III-3.

Fig. 13 Schematic of experimental apparatus when used at Fermilab for a $\nu_\mu e^-$ elastic scattering experiment.

Fig. 14 Schematic diagram of the MWPC.

Fig. 15 Least square fit of a straight line to the electron shower centroids measured by 5 chambers.

Fig. 16 Angular resolution measured with 4 GeV electrons at Cornell University.

Fig. 17 A typical electromagnetic shower induced by a neutrino. Numbers on the horizontal scale label the detector modules. The upper two picture show the y- and x- projection of the shower. The bottom picture shows the pulse height measured by the plastic scintillators in linear scale.

Fig. 18 Schematic illustration of the CCD digitization. The ADC digitizes the charge in each CCD bucket, and the scanner records the CCD bucket number. The CCD is clocked at 50 MHz.

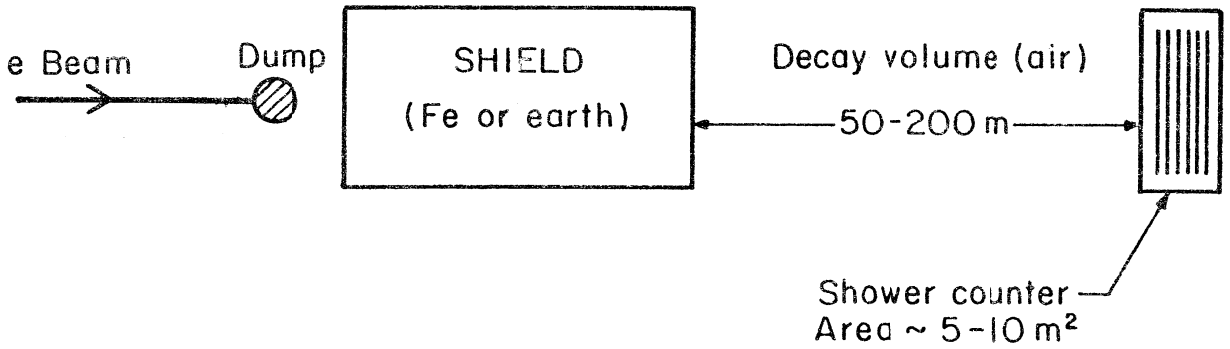
e Beam
Dump
SHIELD
(Fe or earth)
Decay volume (air)
50-200 m
Shower counter
Area ~ 5-10 m²

FIG. 1

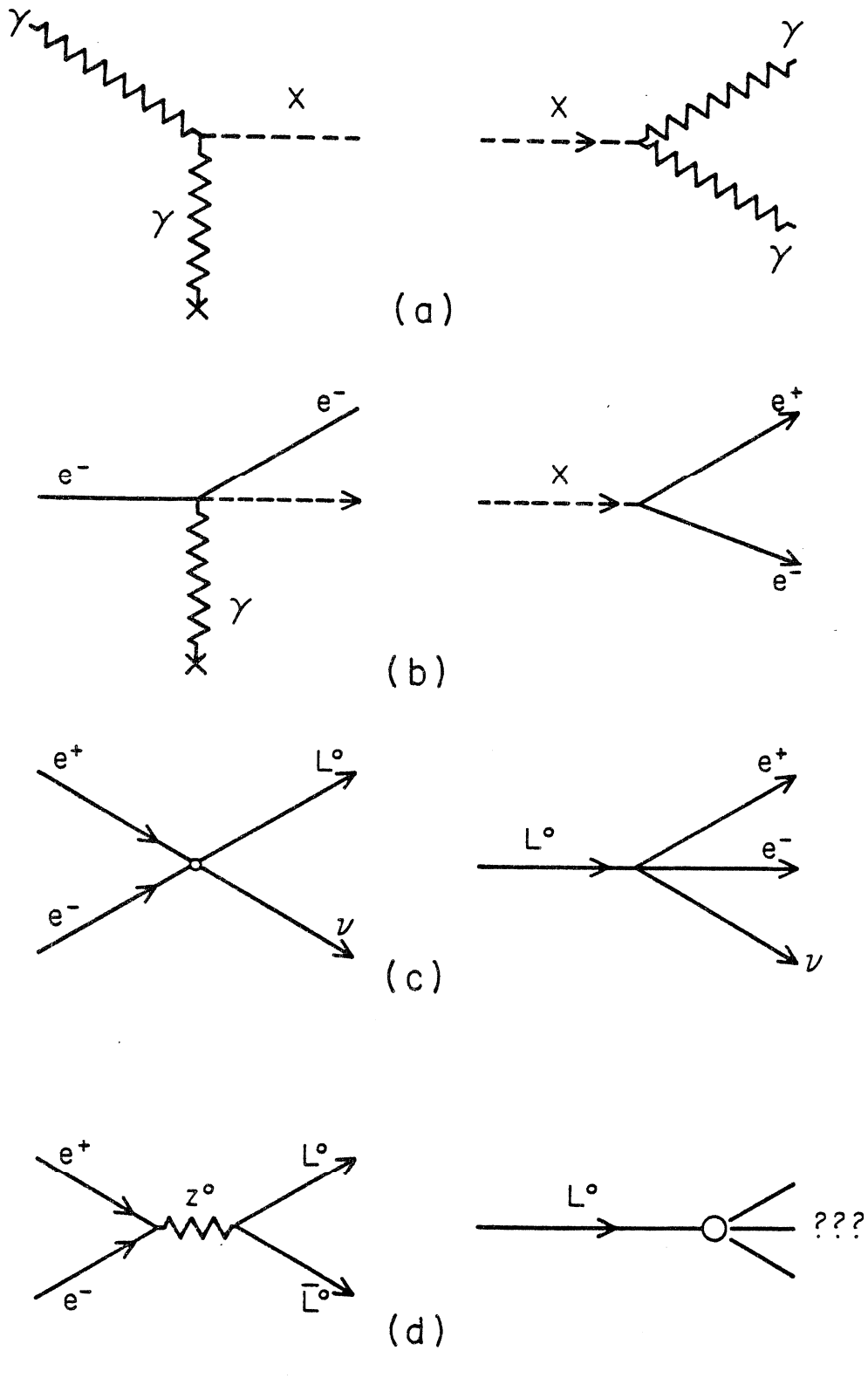

FIG. 2

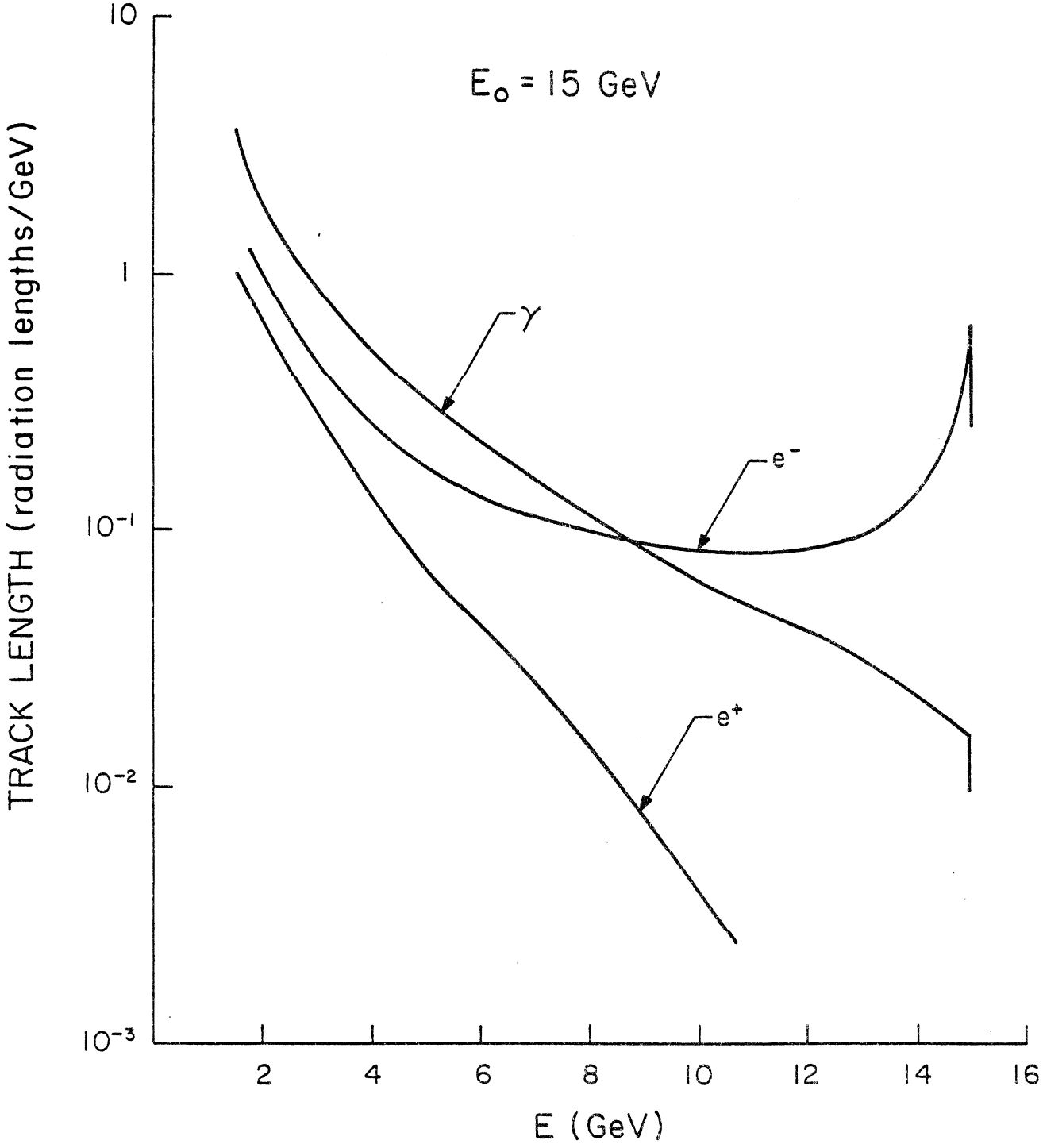
E_o = 15 GeV
TRACK LENGTH (radiation lengths/GeV)
10
1
10^{-1}
10^{-2}
10^{-3}
γ
e^-
e^+
2
4
6
8
10
12
14
16
E (GeV)

FIG. 3a

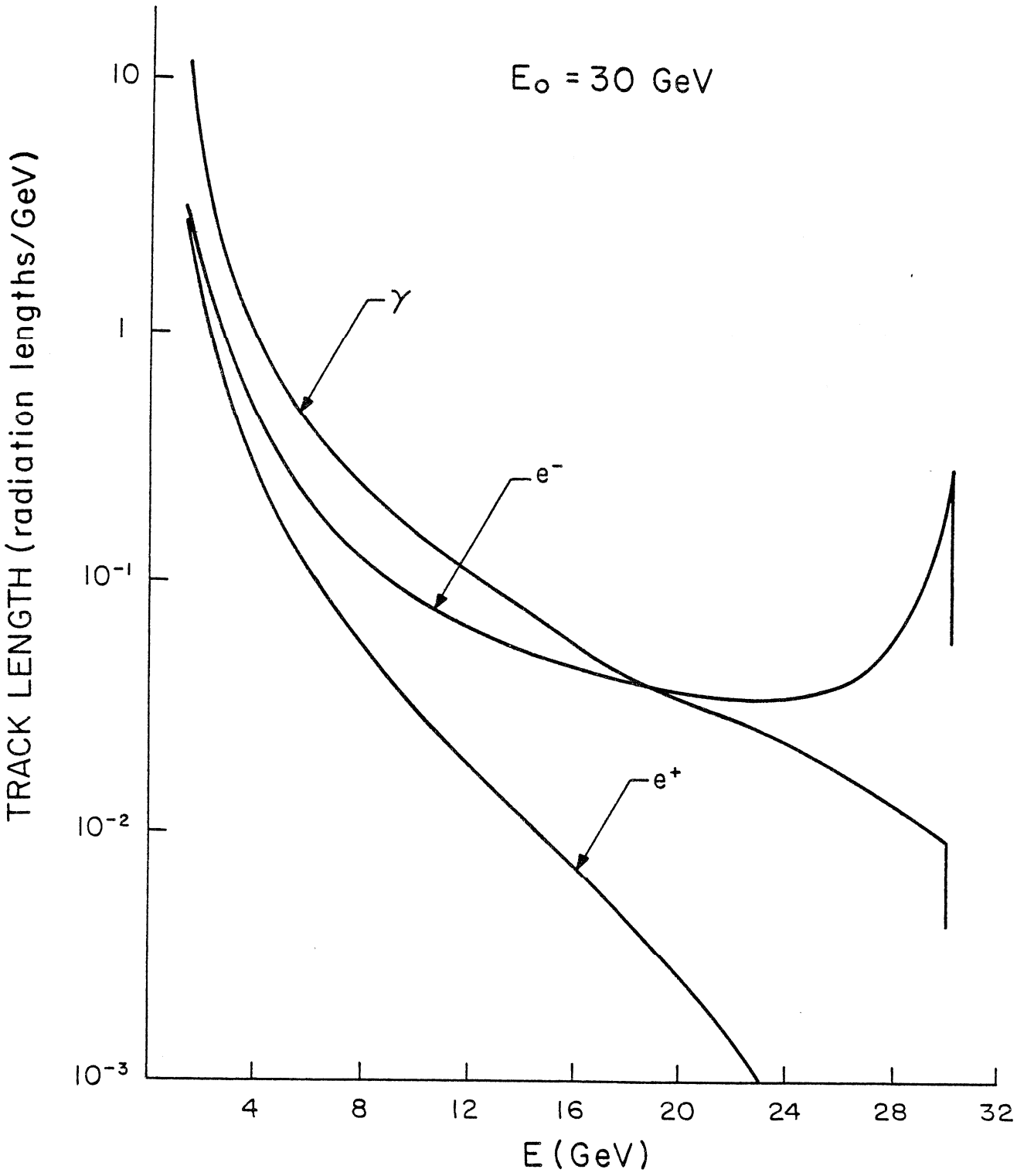
E_o = 30 GeV
TRACK LENGTH (radiation lengths/GeV)
10
1
10^{-1}
10^{-2}
10^{-3}
γ
e^-
e^+
4
8
12
16
20
24
28
32
E (GeV)

FIG. 3b

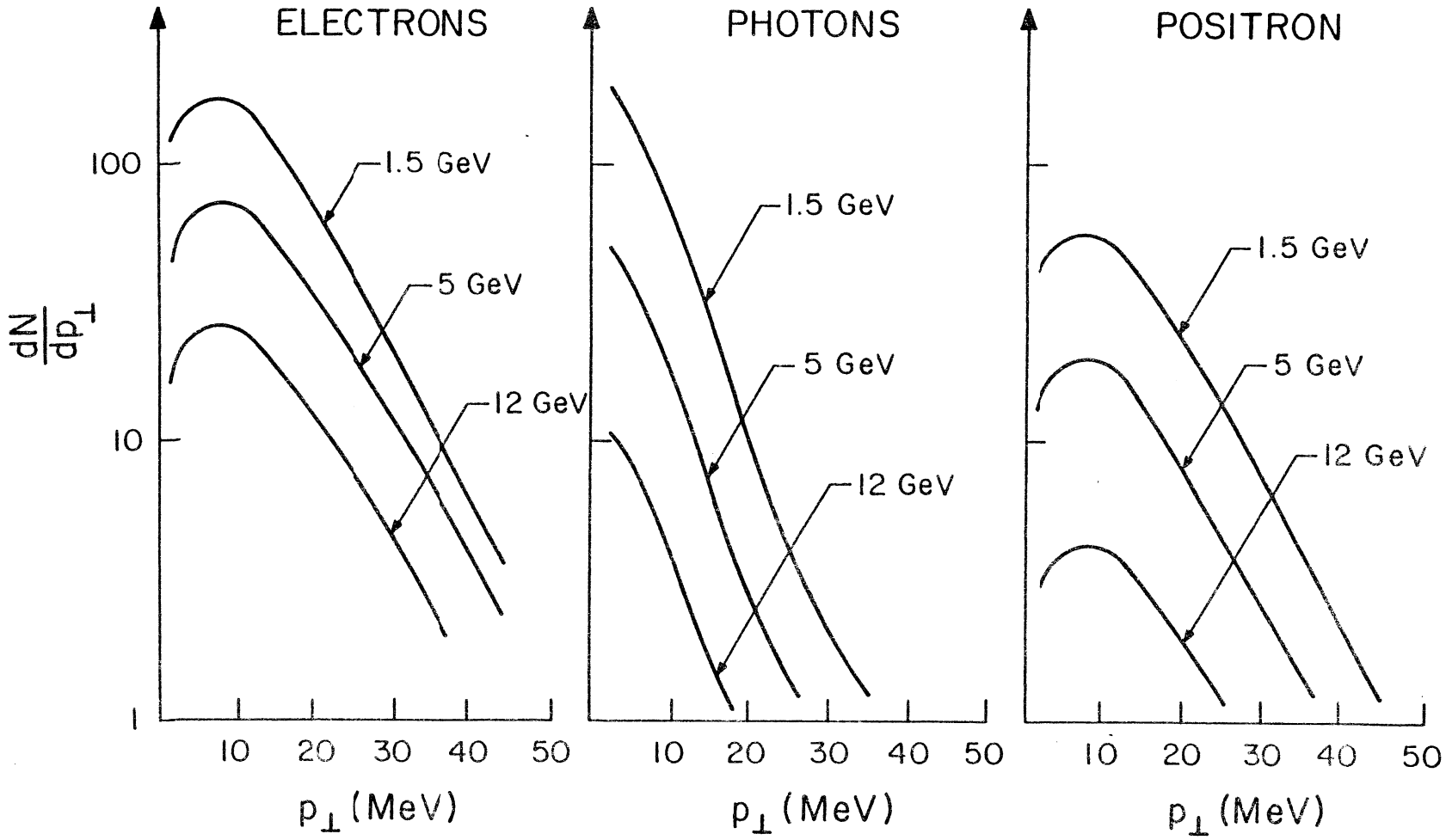
ELECTRONS
PHOTONS
POSITRON
100
10
1
1.5 GeV
5 GeV
12 GeV
$\frac{1}{p_T}\frac{dN}{dp}$
10 20 30 40 50
$p_\perp$ (MeV)

FIG. 4

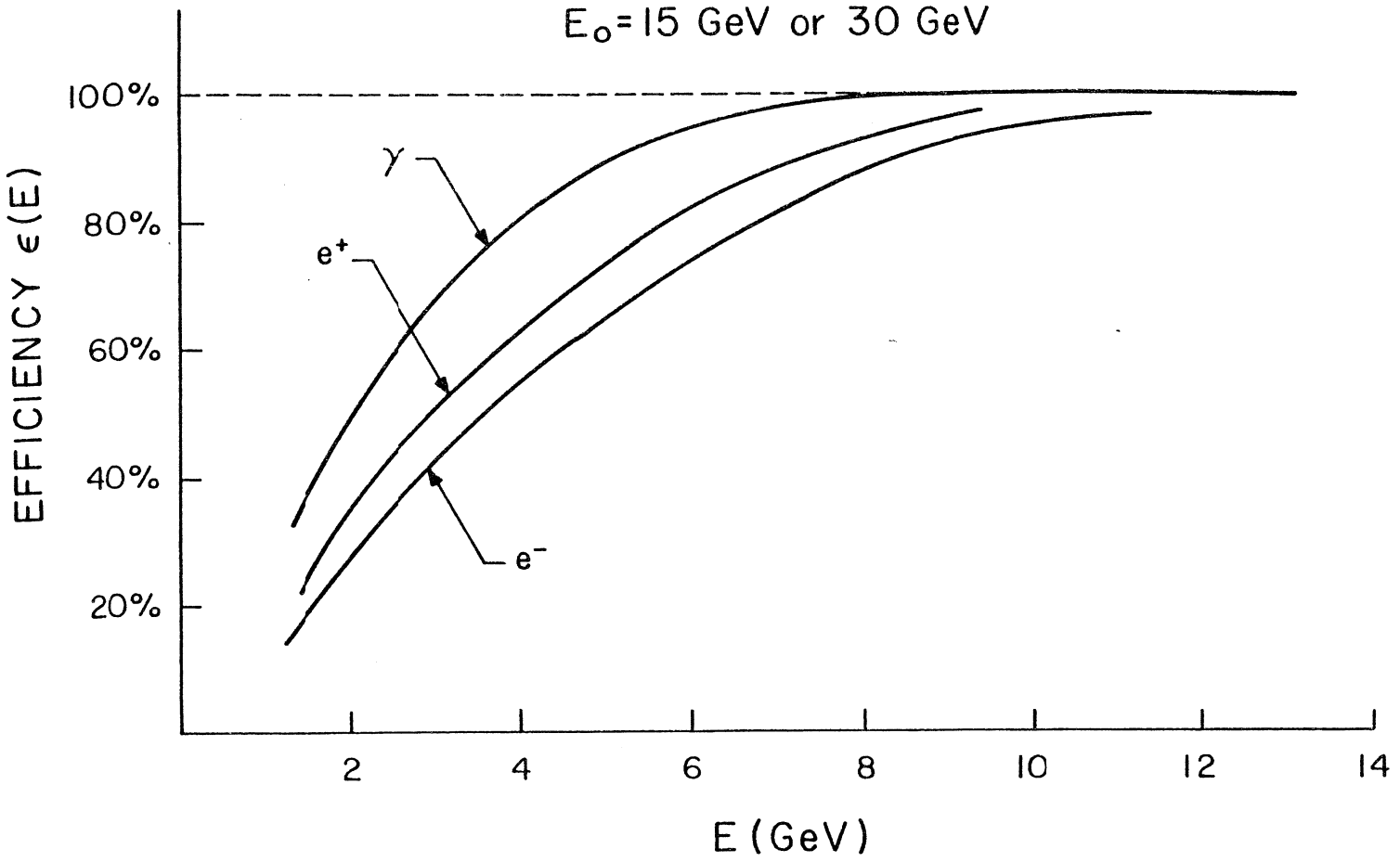
E_o= 15 GeV or 30 GeV
100%
80%
60%
40%
20%
EFFICIENCY ϵ(E)
γ
e+
e−
2
4
6
8
10
12
14
E (GeV)

FIG. 5

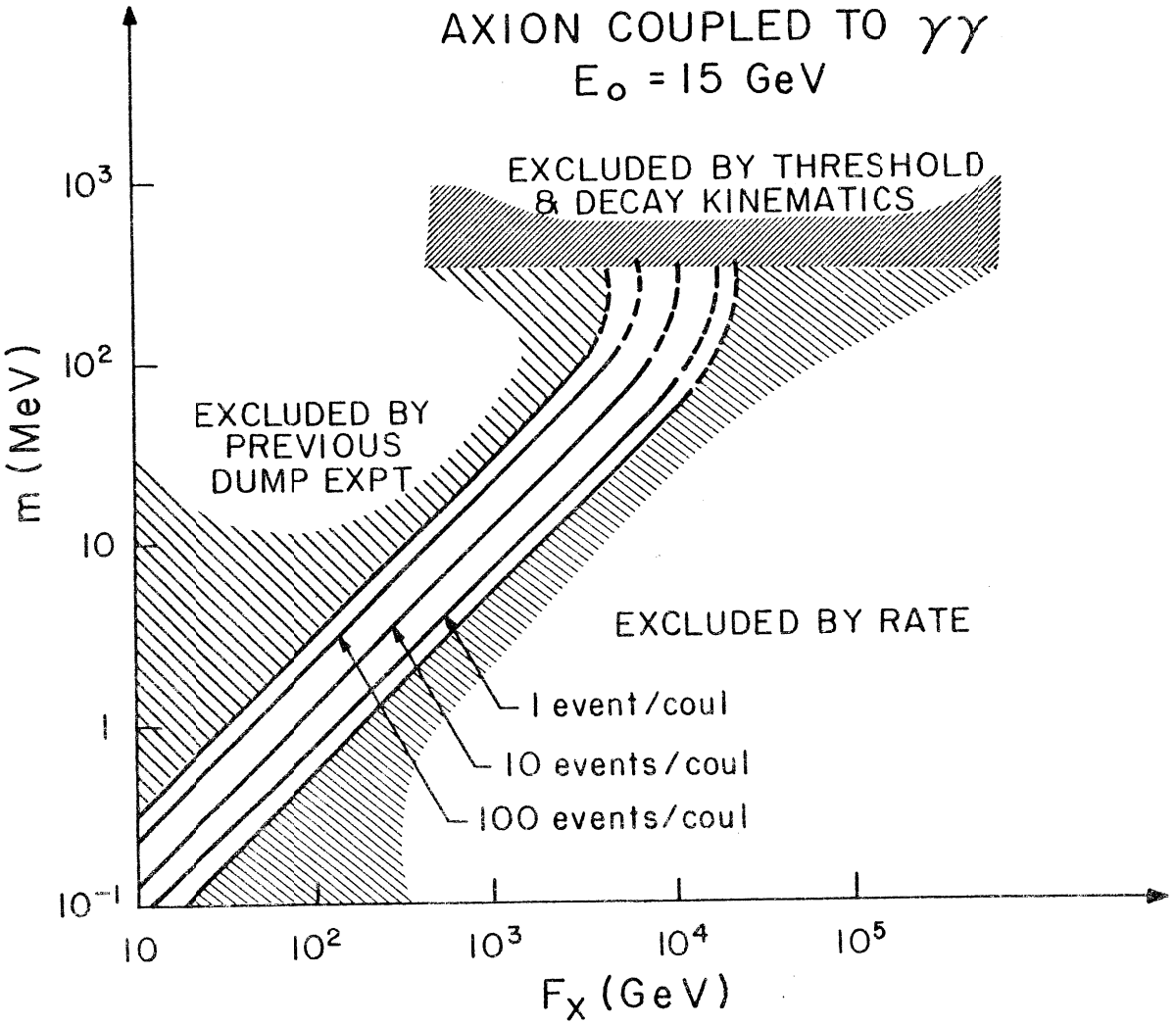
AXION COUPLED TO γγ
E₀ = 15 GeV
EXCLUDED BY THRESHOLD & DECAY KINEMATICS
EXCLUDED BY PREVIOUS DUMP EXPT
EXCLUDED BY RATE
1 event/coul
10 events/coul
100 events/coul
m (MeV)
10³
10²
10
1
10⁻¹
10
10²
10³
10⁴
10⁵
F_X (GeV)

FIG. 6a

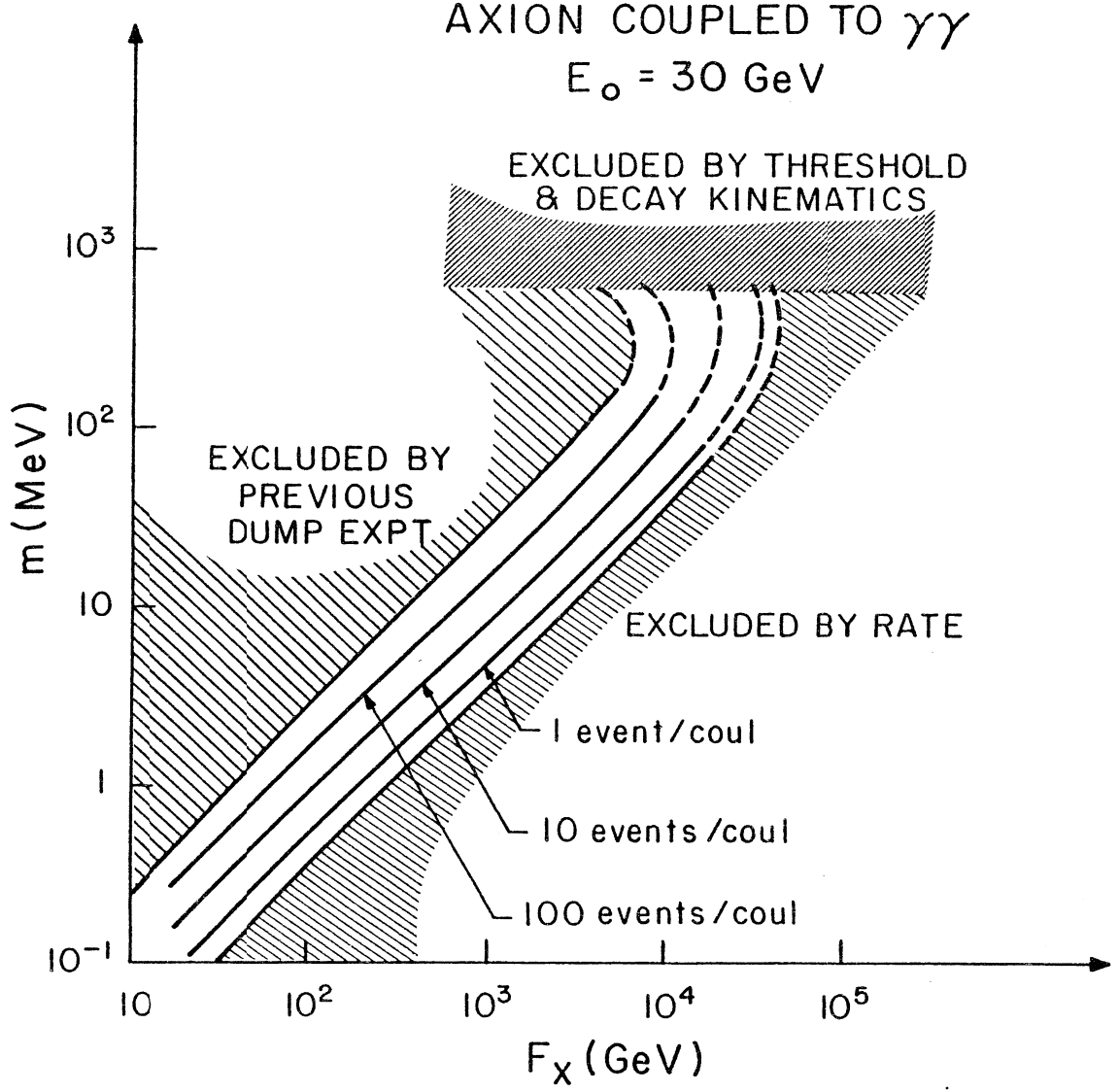
AXION COUPLED TO γγ
E₀ = 30 GeV
EXCLUDED BY THRESHOLD
& DECAY KINEMATICS
EXCLUDED BY
PREVIOUS
DUMP EXPT
EXCLUDED BY RATE
1 event/coul
10 events/coul
100 events/coul
m (MeV)
10³
10²
10
1
10⁻¹
10
10²
10³
10⁴
10⁵
F_X (GeV)

FIG. 6b

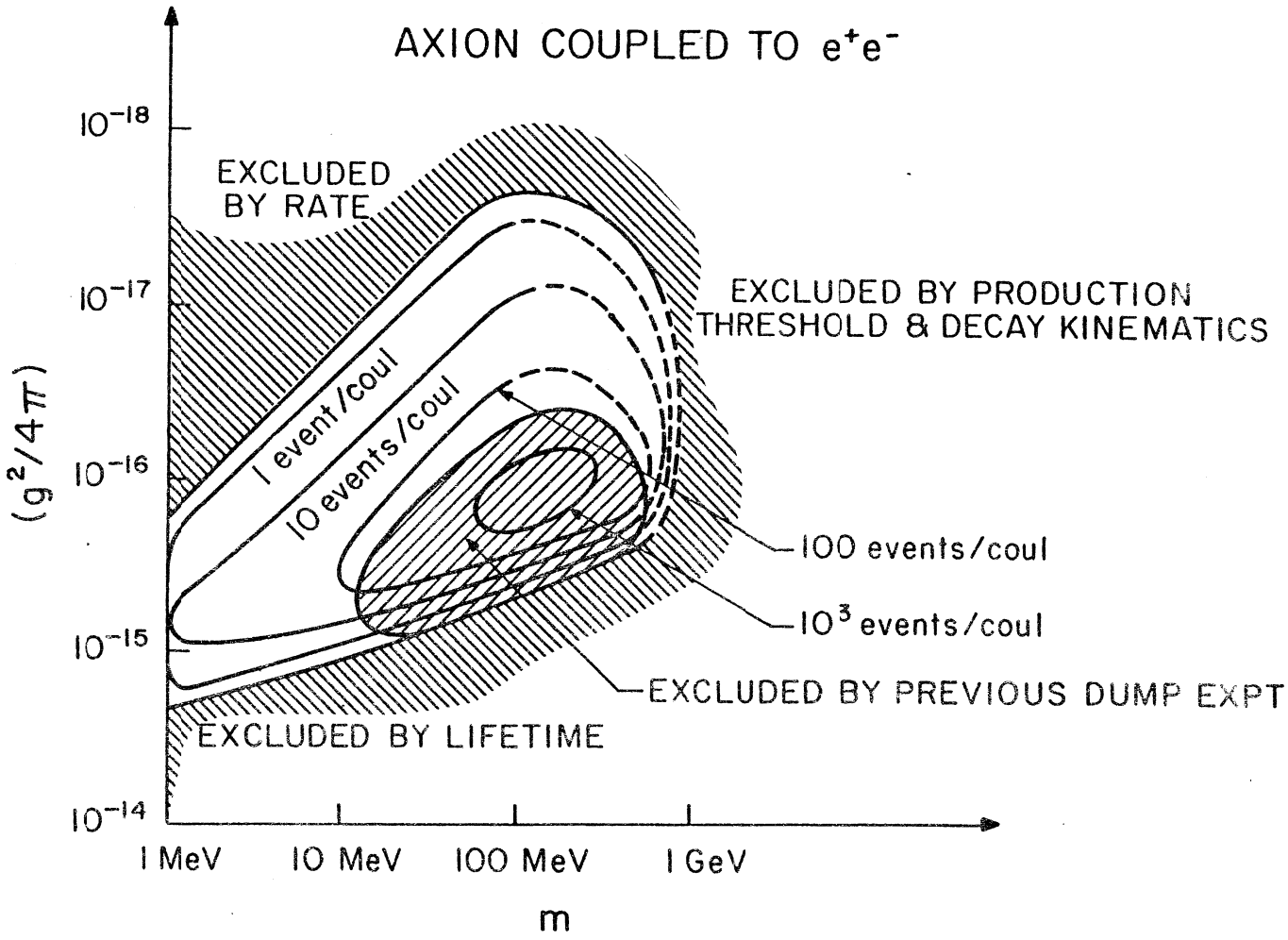
AXION COUPLED TO e^+e^-
10^{-18}
10^{-17}
10^{-16}
10^{-15}
10^{-14}
$(g^2/4\pi)$
EXCLUDED BY RATE
EXCLUDED BY PRODUCTION THRESHOLD & DECAY KINEMATICS
1 event/coul
10 events/coul
100 events/coul
10^3 events/coul
EXCLUDED BY PREVIOUS DUMP EXPT
EXCLUDED BY LIFETIME
1 MeV
10 MeV
100 MeV
1 GeV
m

FIG. 7

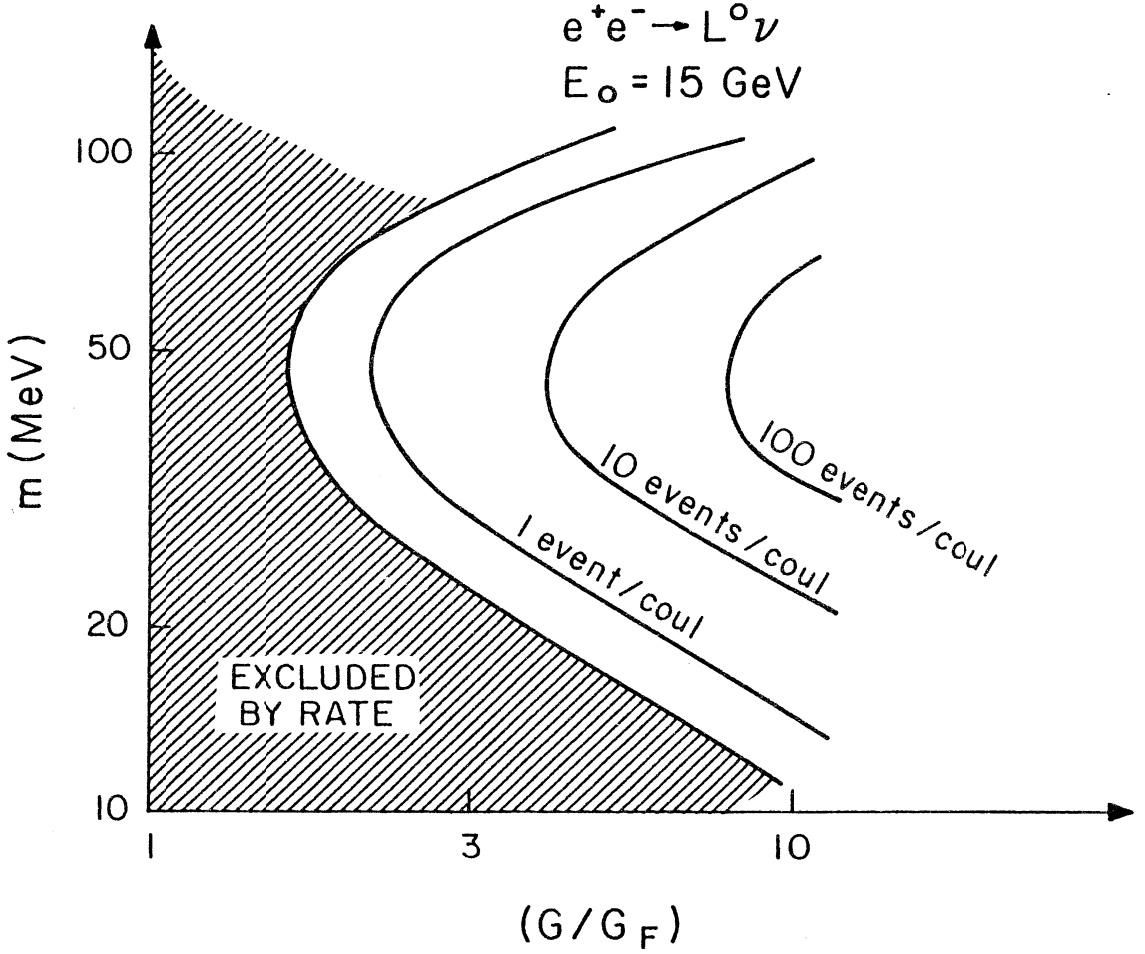
$e^+e^- \rightarrow L^o\nu$
$E_o = 15$ GeV
100
50
20
10
m (MeV)
EXCLUDED BY RATE
1 event/coul
10 events/coul
100 events/coul
1
3
10
(G/G_F)

FIG. 8a

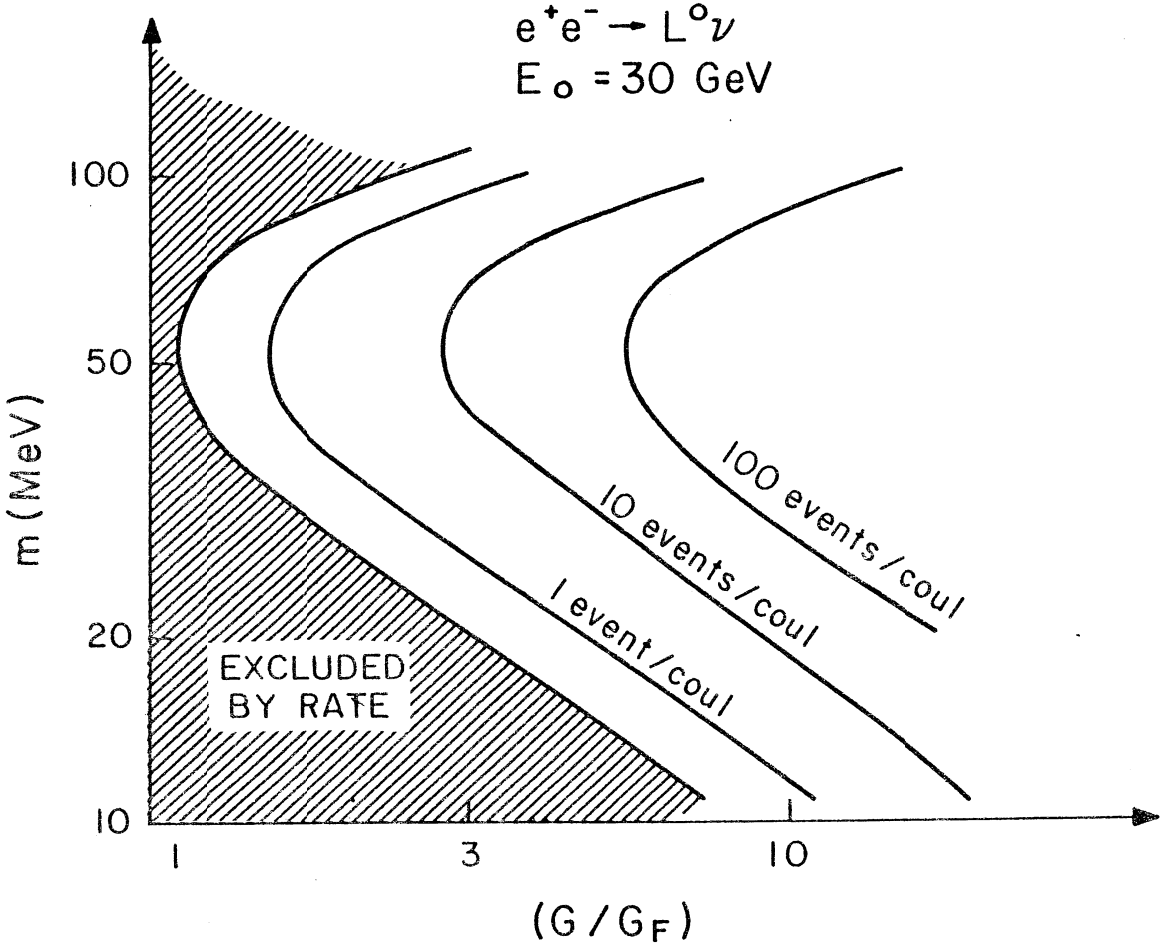
$e^+e^- \rightarrow L^o\nu$
$E_o = 30$ GeV
100
50
20
10
m (MeV)
EXCLUDED BY RATE
1 event/coul
10 events/coul
100 events/coul
1
3
10
(G/G_F)

FIG. 8b

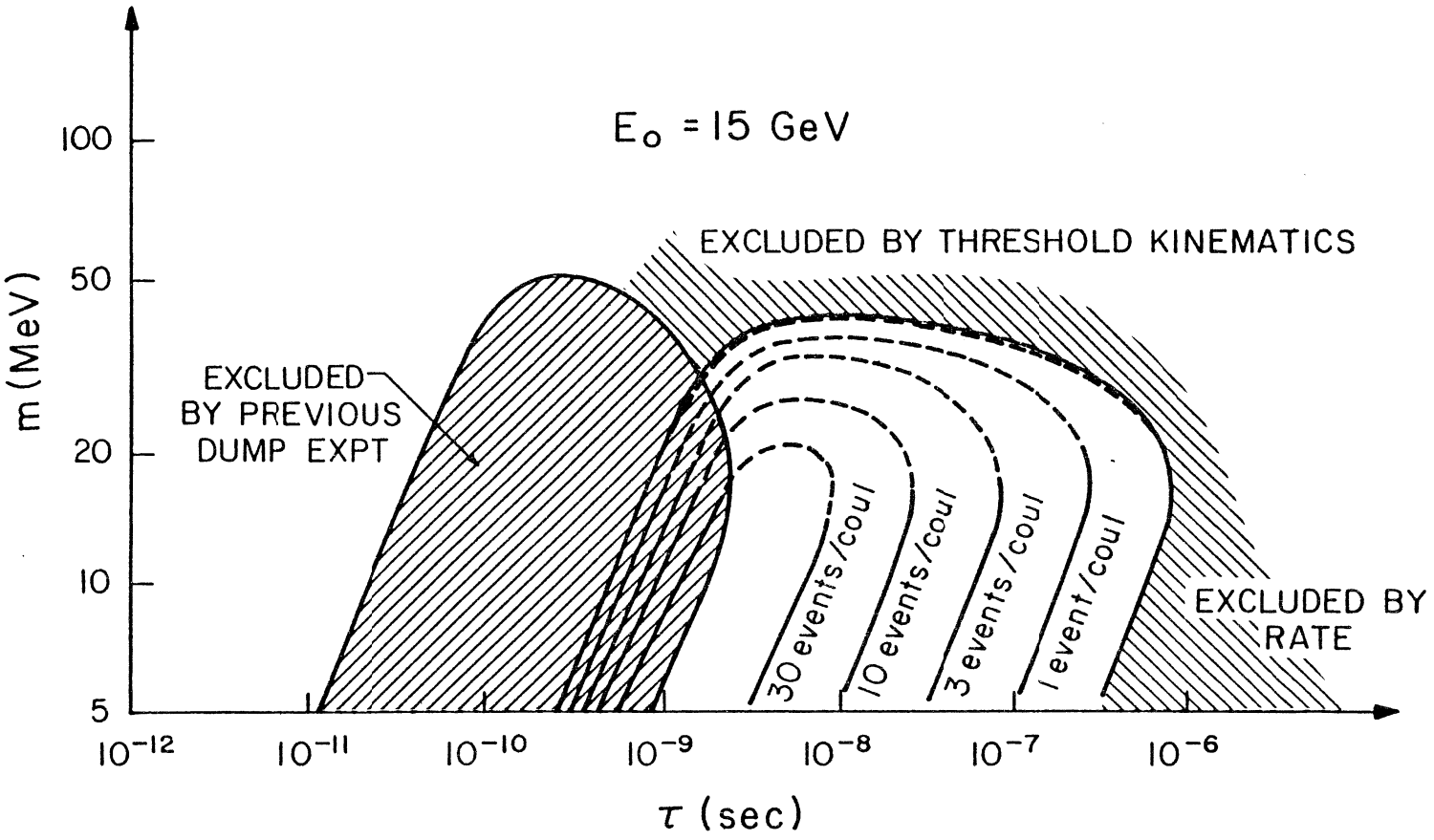
E_o = 15 GeV
EXCLUDED BY THRESHOLD KINEMATICS
EXCLUDED BY PREVIOUS DUMP EXPT
30 events/coul
10 events/coul
3 events/coul
1 event/coul
EXCLUDED BY RATE
m (MeV)
100
50
20
10
5
10^{-12}
10^{-11}
10^{-10}
10^{-9}
10^{-8}
10^{-7}
10^{-6}
τ (sec)

FIG. 9a

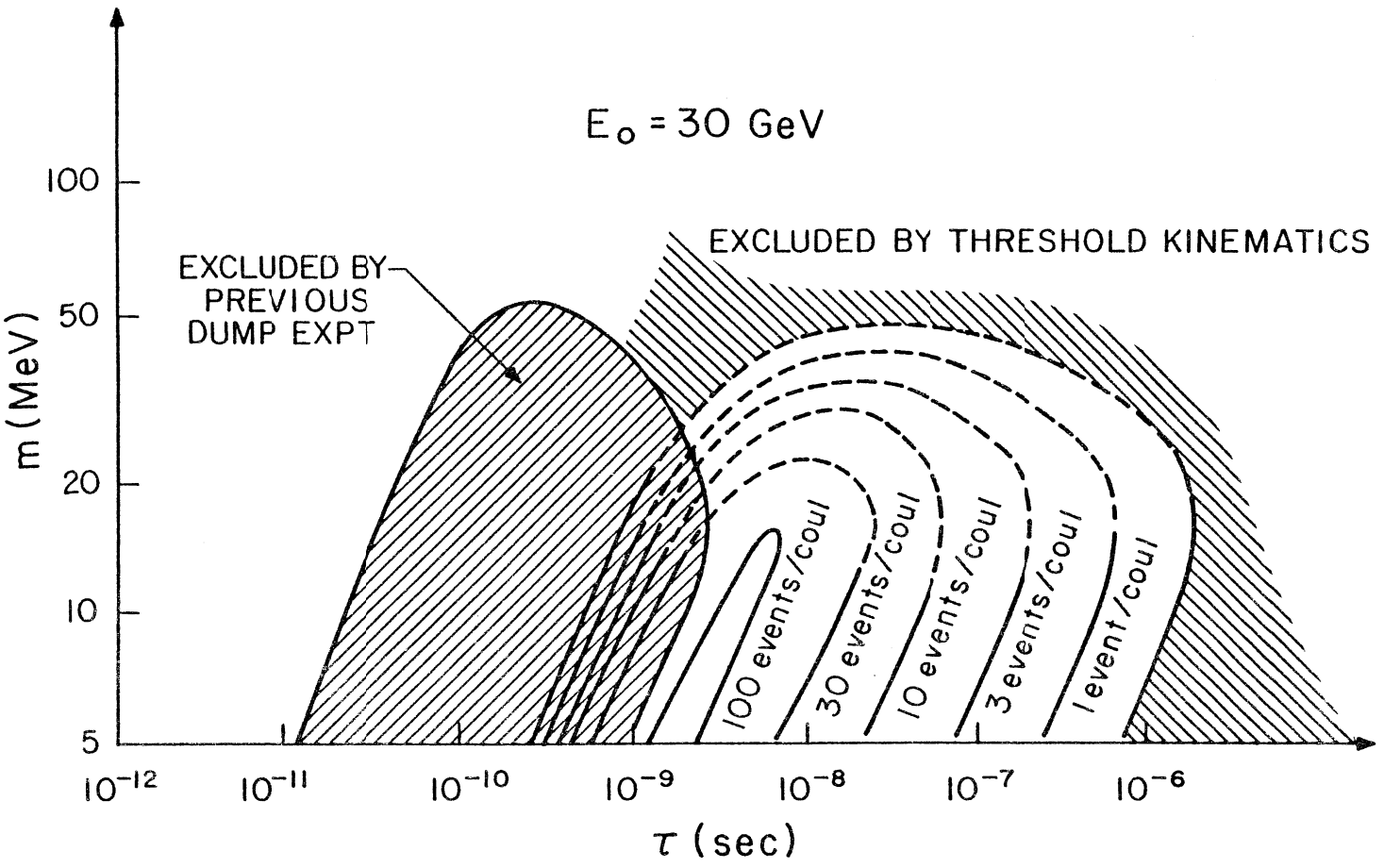
$E_o = 30$ GeV
EXCLUDED BY THRESHOLD KINEMATICS
EXCLUDED BY PREVIOUS DUMP EXPT
100 events/coul
30 events/coul
10 events/coul
3 events/coul
1 event/coul
m (MeV)
100
50
20
10
5
10^{-12}
10^{-11}
10^{-10}
10^{-9}
10^{-8}
10^{-7}
10^{-6}
τ (sec)

FIG. 9b

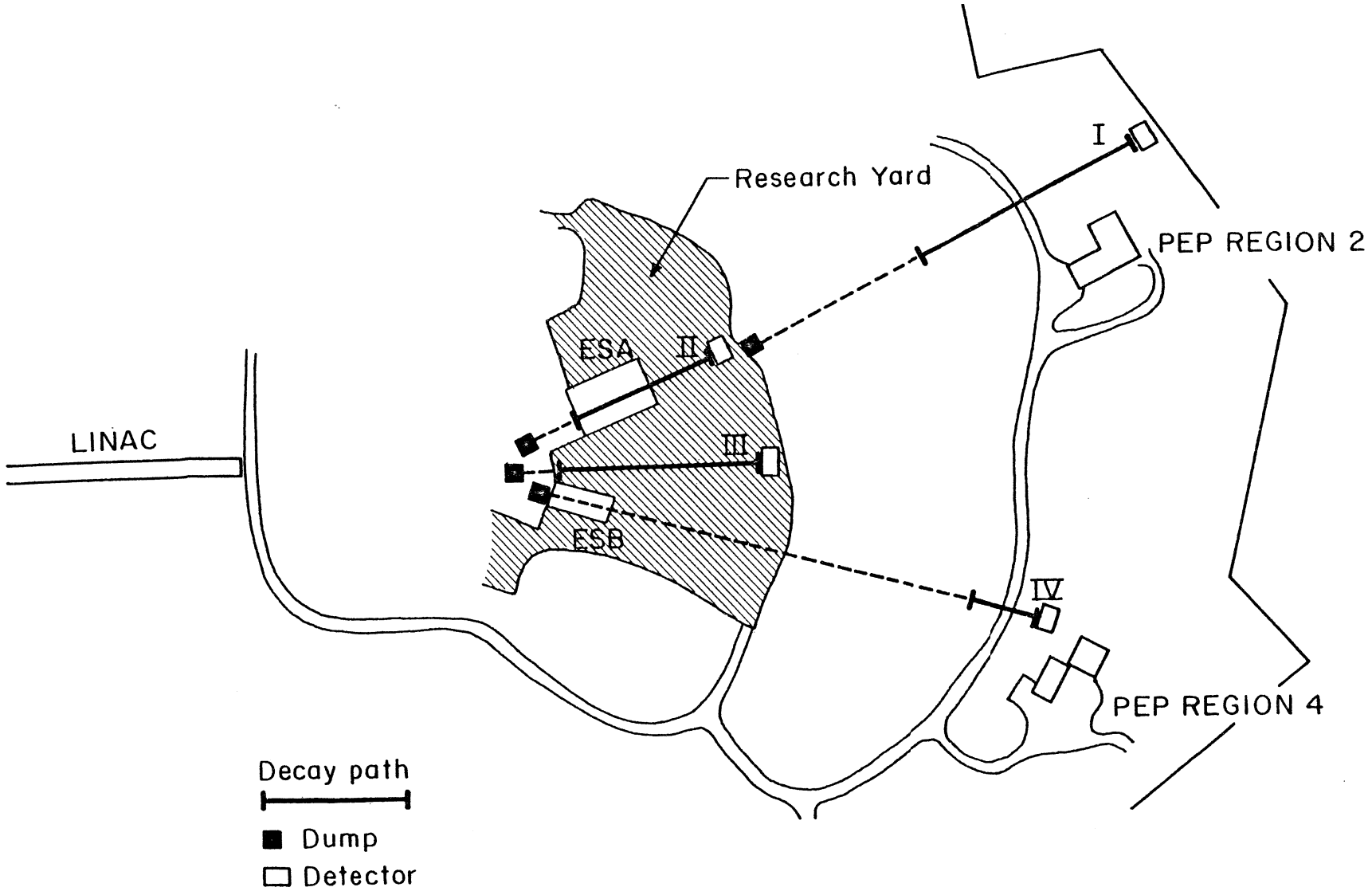
I
Research Yard
PEP REGION 2
ESA
II
LINAC
III
ESB
IV
PEP REGION 4
Decay path
Dump
Detector

FIG. 10

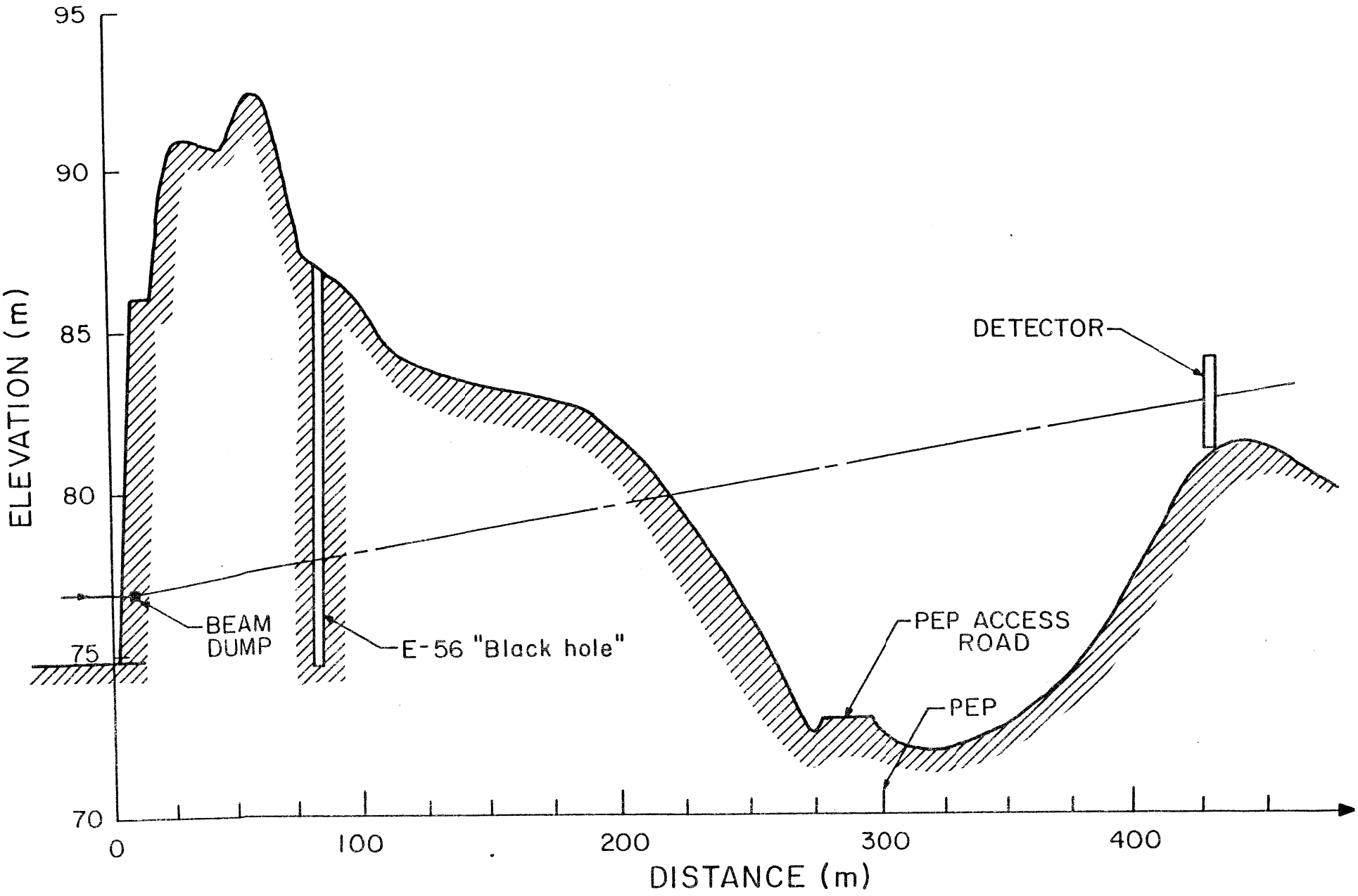
95
90
85
80
75
70
ELEVATION (m)
DETECTOR
BEAM
DUMP
E-56 "Black hole"
PEP ACCESS
ROAD
PEP
0
100
200
300
400
DISTANCE (m)

FIG. 11

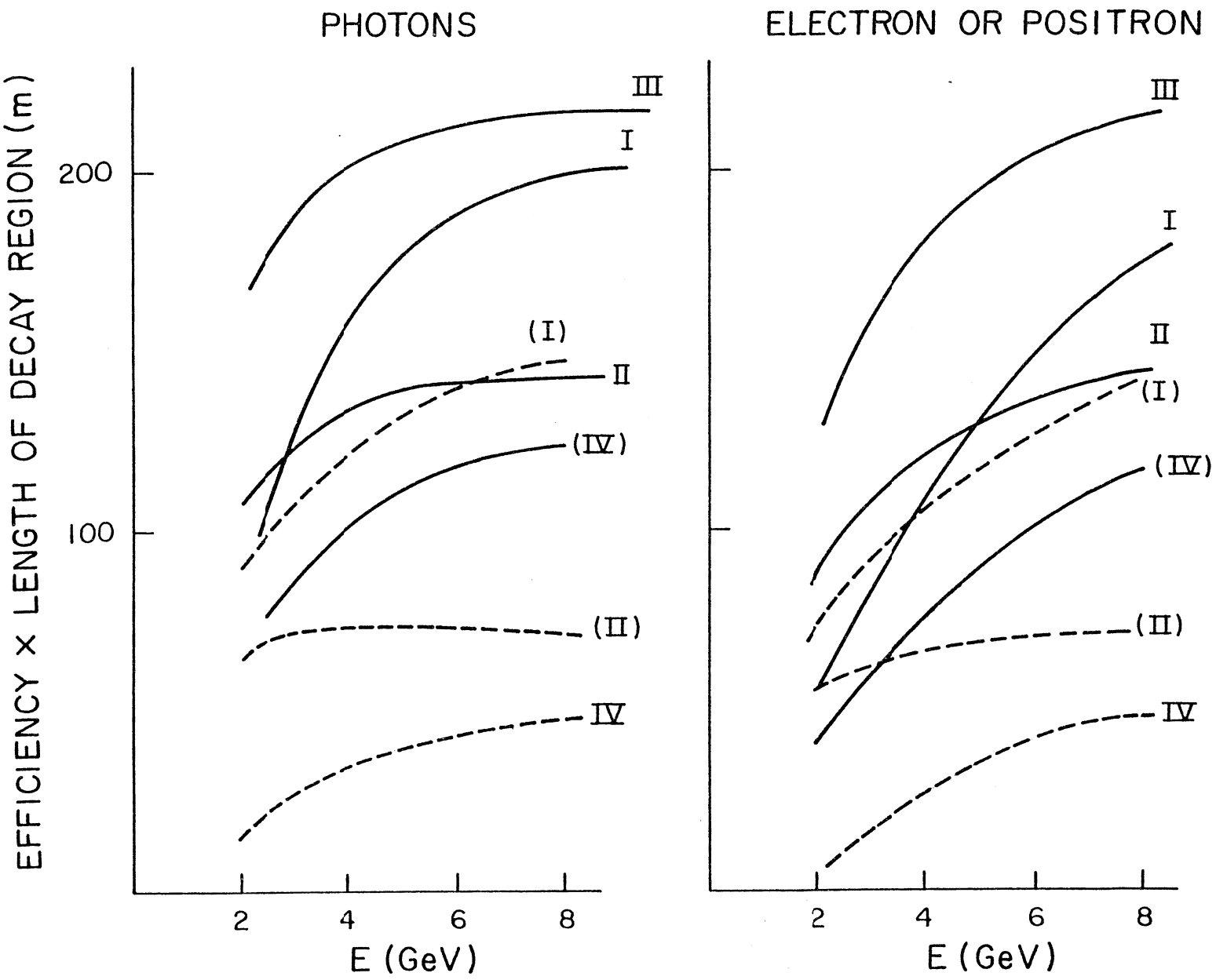
PHOTONS
ELECTRON OR POSITRON
EFFICIENCY × LENGTH OF DECAY REGION (m)
200
100
III
I
(I)
II
(IV)
(II)
IV
2
4
6
8
E (GeV)

FIG. 12

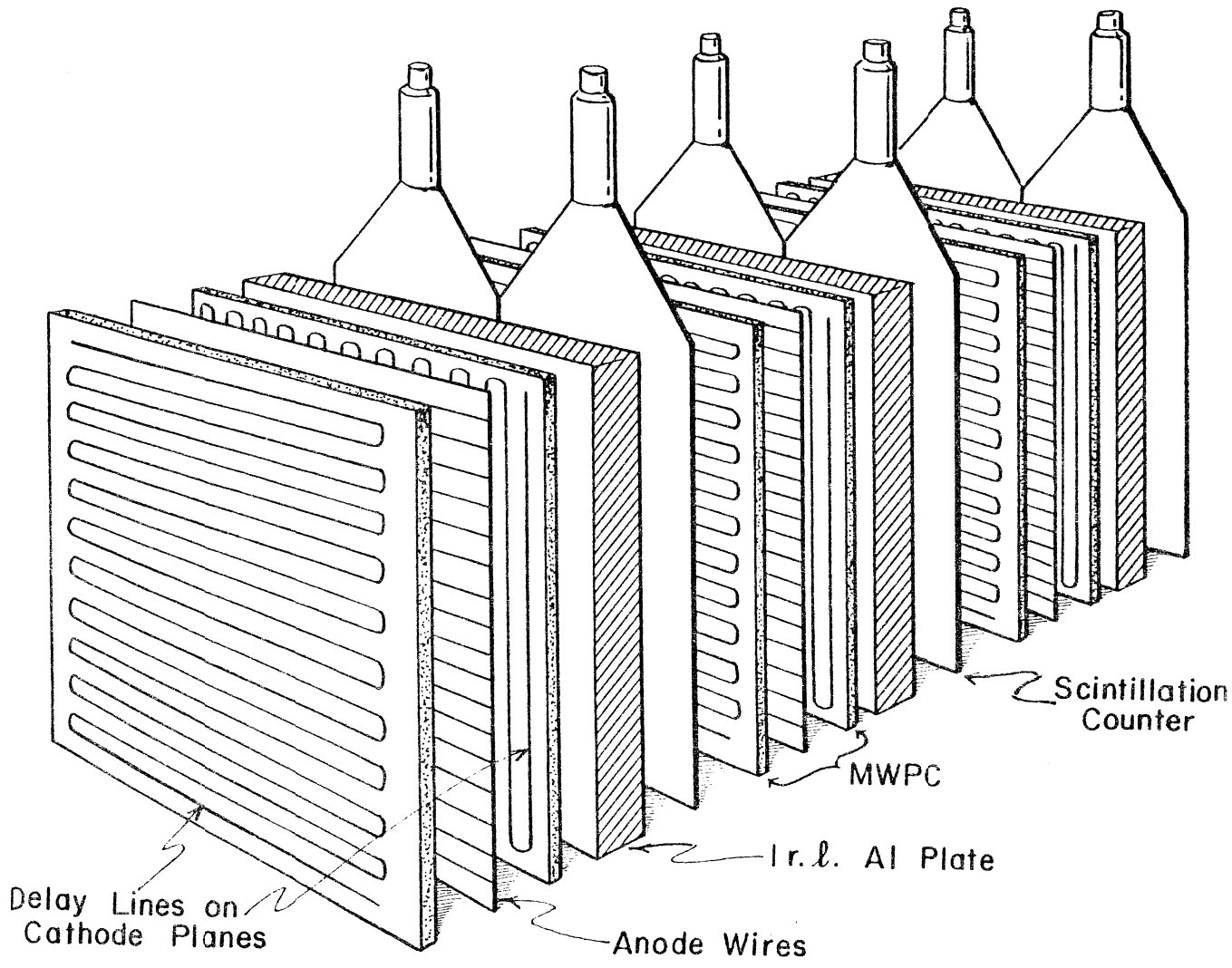
Scintillation Counter
MWPC
1r.ℓ. Al Plate
Delay Lines on Cathode Planes
Anode Wires

FIG. 13

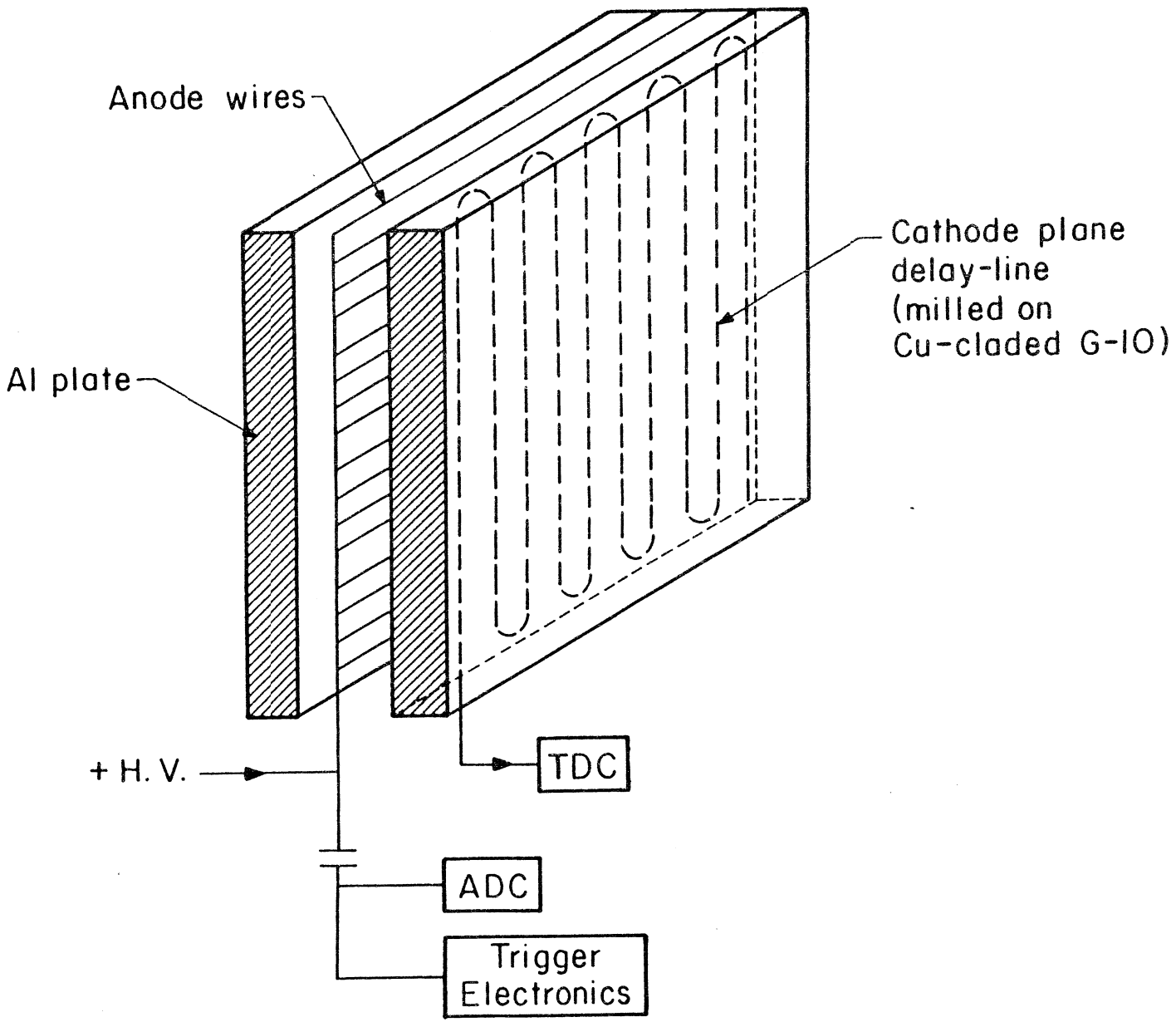
Anode wires
Cathode plane
delay-line
(milled on
Cu-cladded G-10)
Al plate
+ H. V.
TDC
ADC
Trigger
Electronics

FIG. 1

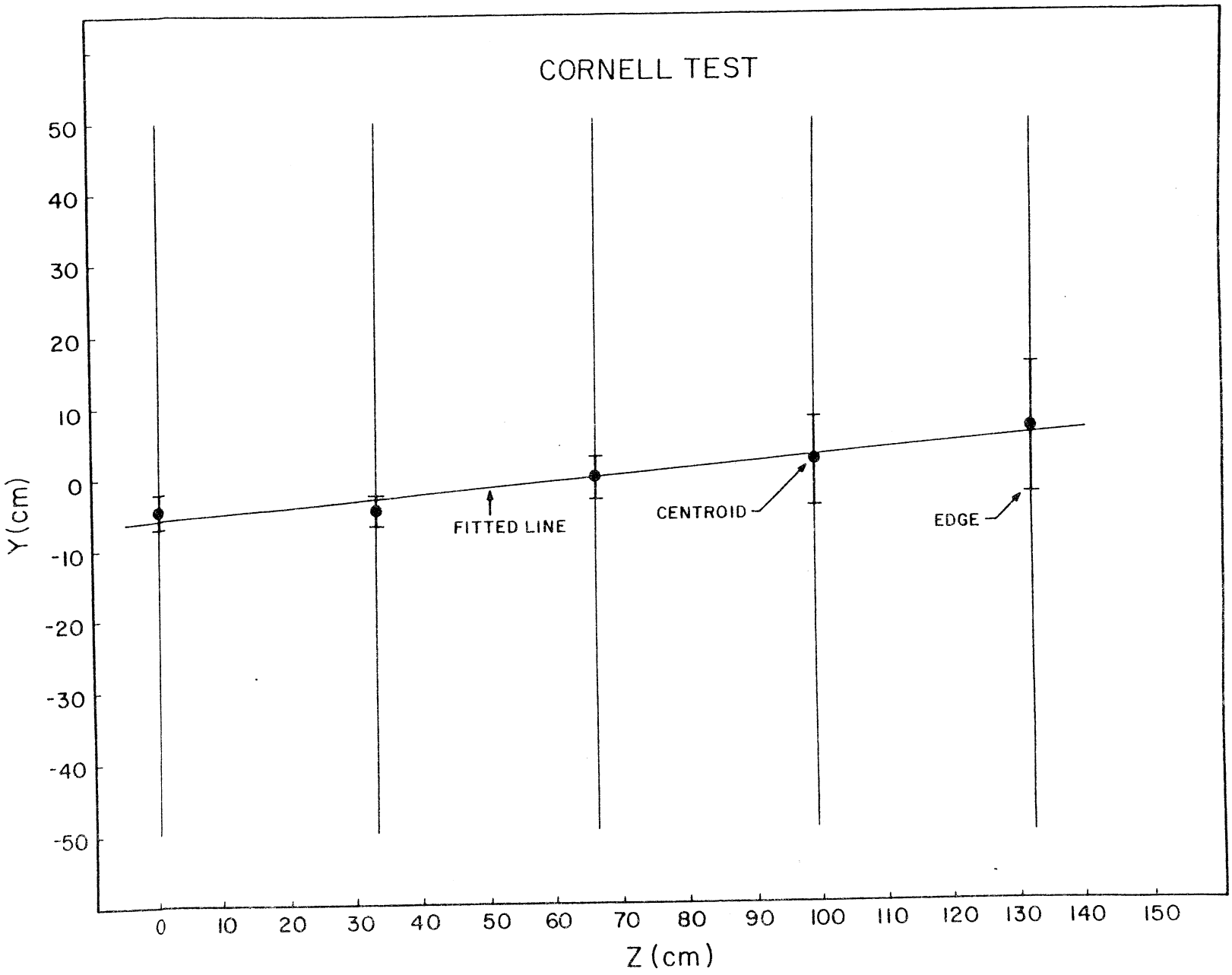
CORNELL TEST
50
40
30
20
10
0
-10
-20
-30
-40
-50
Y (cm)
0
10
20
30
40
50
60
70
80
90
100
110
120
130
140
150
Z (cm)
FITTED LINE
CENTROID
EDGE

FIG. 15

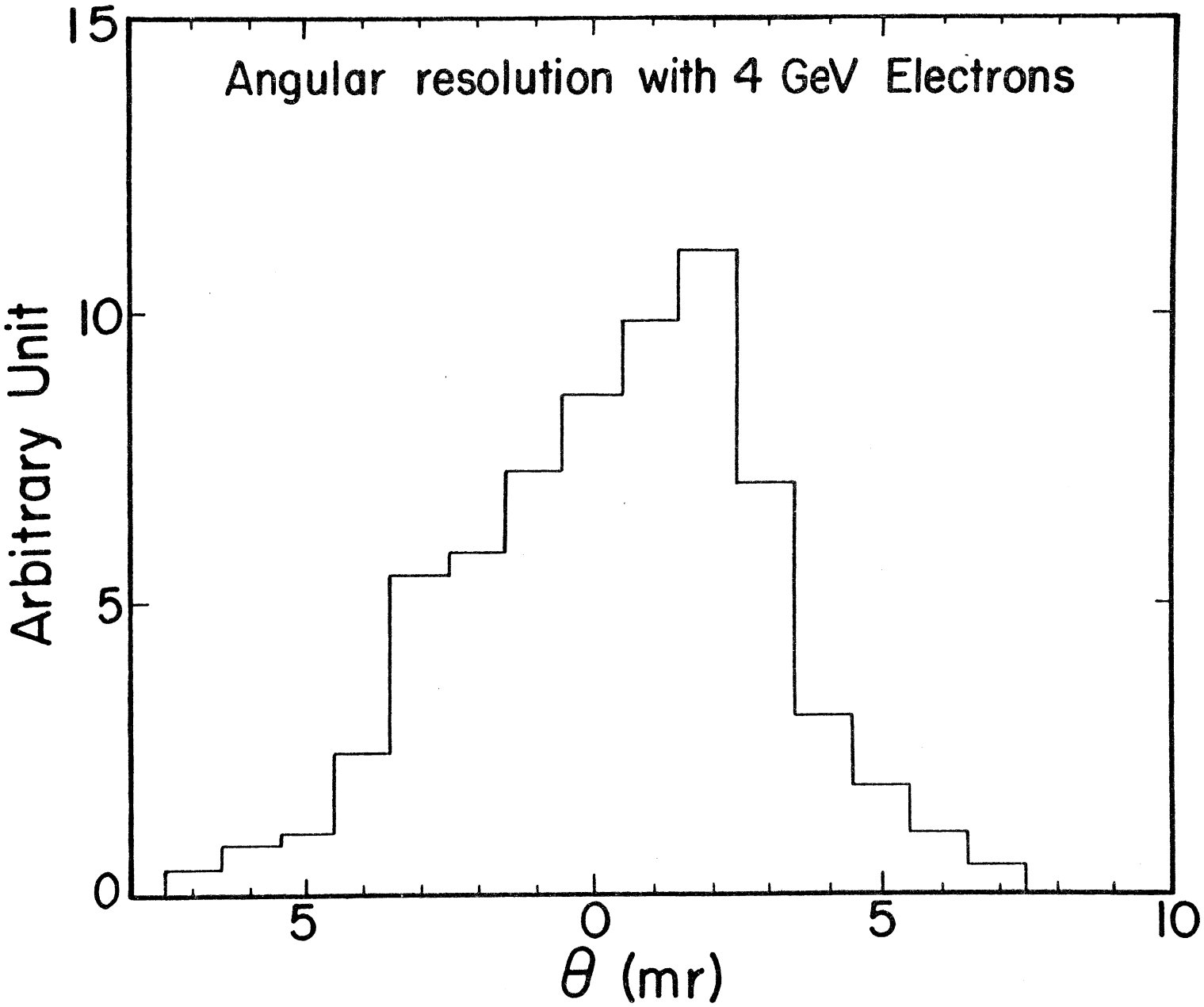
Angular resolution with 4 GeV Electrons
Arbitrary Unit
15
10
5
0
5
0
5
10
θ (mr)

FIG. 16

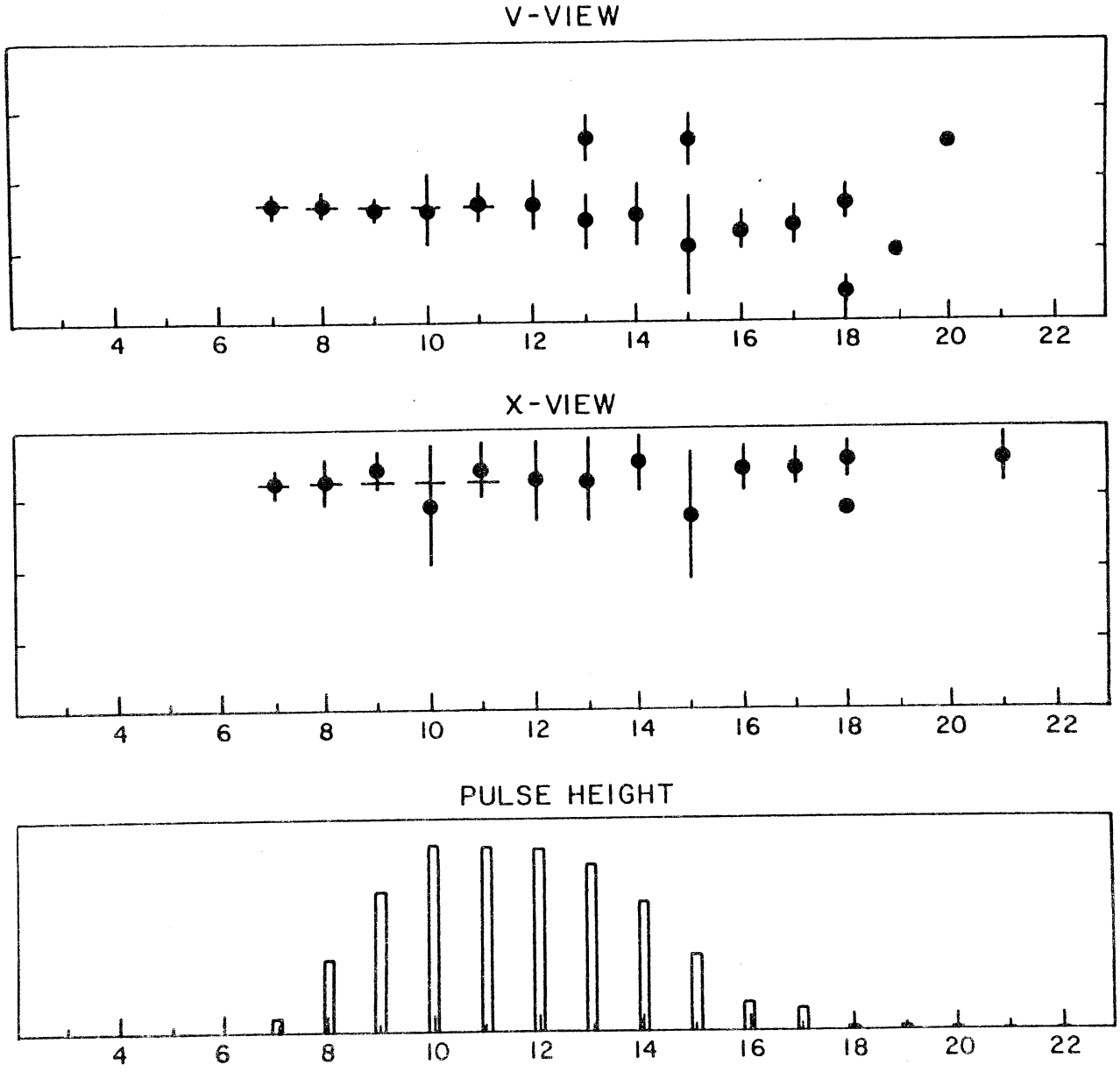
V-VIEW
4
6
8
10
12
14
16
18
20
22
X-VIEW
4
6
8
10
12
14
16
18
20
22
PULSE HEIGHT
4
6
8
10
12
14
16
18
20
22

FIG. 17

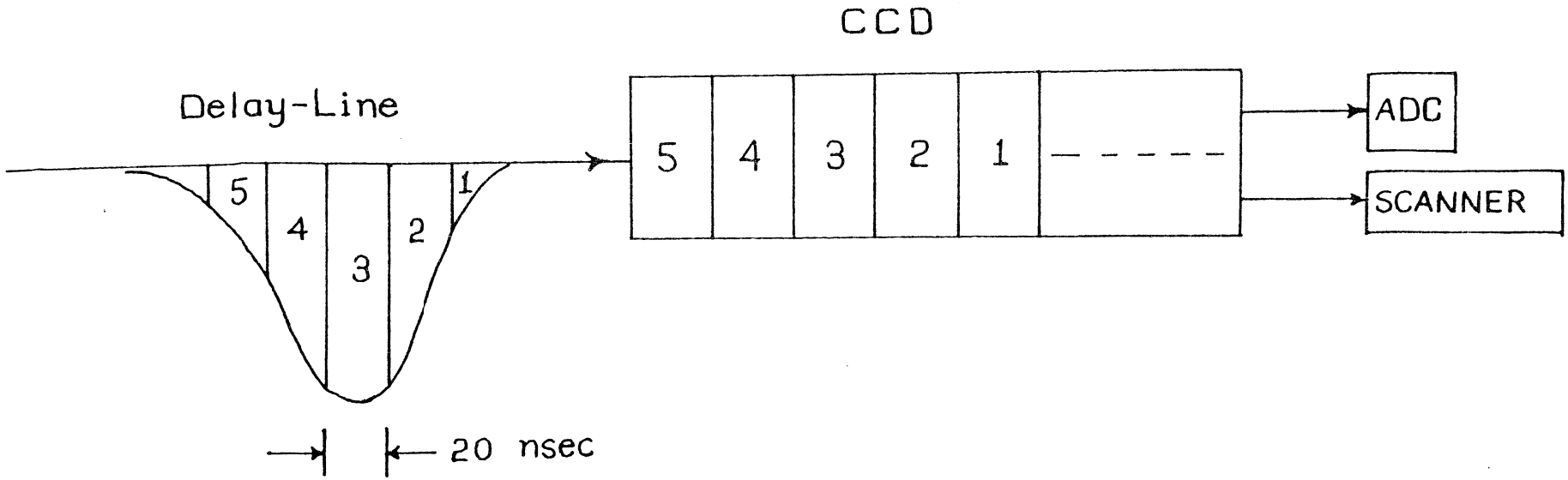

FIG. 18

VPI-HEP-80/3
February 1980

Appendix 1

An Electromagnetic Shower Detector Using Proportional Wire Chambers With Cathode Plane Delay-Line Readout*

Thomas A. Nunamaker, Richard H. Heisterberg, and Luke W. Mo

Department of Physics

Virginia Polytechnic Institute and State University

Blacksburg, VA 24061

*Supported by National Science Foundation under Grant No. PHY-7727521

Accepted for publication in Nucl. Inst. and Meth., 1980

ABSTRACT

The construction and performance of a fine-grained electromagnetic shower detector is described. The detector consisted of 49 1m x 1m proportional wire chambers interlaced with one radiation length thick Aluminum plates. The delay-line readout on the cathode planes measured the centroid positions of the shower. The anode wire planes measured the shower energy and can be used to form an experimental trigger. The detector was used successfully in an elastic neutrino-electron scattering experiment at Fermilab.

In experimental high energy physics, it is most desirable to have a fine-grained electromagnetic shower detector which can measure both the angle and the energy of the shower with high precision. Because the detector size is necessarily large, economy becomes an important consideration. In this paper, we will report a satisfactory solution for building such a detector. A detector assembly 1m x 1m in cross section and 49 r.ℓ. in depth was built, and used successfully in an experiment at Fermilab to study the reaction $\nu_\mu + e^- \rightarrow \nu_\mu + e^-$.[1] In order to search for these events from a very high background, good angular resolution of the detector is mandatory. The angular resolution achieved with the detector was $\pm$ 5 mr.

Basically, the detector was made of 49 modules. Each module consisted of one Aluminum radiator of $\sim$1 r.ℓ. in thickness, and one multiple-wire proportional chamber (MWPC). The anode wires of each chamber were electrically connected together with the common pulses fed to an analogue-to-digital converter (ADC) to measure the energy deposition in each layer of the detector. On the two cathode planes, zigzag delay-lines of spacing 1.5 mm along orthogonal directions were equipped to measure both the x- and y-positions of the shower from tap points as time intervals. There were five taps, equi-distantly spaced, along each of the two orthognal edges of the chamber. Signals from the taps were digitized by time-to-digital converters (TDC's) of the start-stop type, which had a range of 1,000 nsec and a time-resolution of 1 nsec.

In the following sections, we will describe the construction and performance of the MWPC's.

I. Construction of the MWPC

The cathode planes of the MWPC were made from 1/4" thick Aluminum jig plate. Copper-clad G-10 sheets were first milled into a zigzag delay-line configuration, and then glued onto the Aluminum plate. G-10 spacers attached to one aluminum plate were used to support the anode wire plane, which were made of gold-plated tungsten wires of 20μ in diameter, spaced 3 mm apart. The spacing between the anode plane and the cathode plane was 1/4". The detailed arrangement of the chamber is shown in Figure 1.

The chambers were filled with a gas mixture of 80% CO_2, 19.7% Argon, and 0.3% Freon-13-B1, and were operated at a typical positive high voltage of ∿2,800 volts on the anode planes. The cathode planes were at ground potential. To protect the anode wires from sparking damage, every group of 8 anode wires was connected to the H.V. power supply through a 10 mega-ohm resistor. As shown in Figure 2, the anode wires were soldered to a 1/64" thick copper clad G-10 strip which acted as the high frequency coupling capacitor for the outgoing fast signal from the anode. One side of the G-10 strip collected signals from each anode wire, and the other side carried the capacitively coupled signal to an amplifier through an H.V. decoupling capacitor.

The delay-line on the cathode planes had a characteristic impedance of ∿100 ohms. Between two tap points, the propagation time was ∿500 nsec, corresponding to a transverse distance of 250 mm. It was found that the signal was attenuated by ∿x2 between neighboring taps. The dispersion and attenuation characteristics of the delay-line for a step signal are shown in Figure 3.

II. Performance of the Detector

An assembly of 49 chambers were built and used in a neutrino-electron scattering experiment at Fermilab. A photograph of the setup is shown in Figure 4. In this experiment, the anode signals from six consecutive chambers were used to form an experimental trigger which indicated the occurence of an electromagnetic shower. Each anode signal was also individually digitized for later data analysis.

A portion of the apparatus consisting of 5 modules was tested using 2.5 - 9.5 GeV electrons at Cornell University, and a 10 module section for 5 - 30 GeV electrons and pions at Fermilab. The angular resolution and the energy calibration are shown in Figures 5 and 6. The angular resolution is approximately $\pm$ 5 mr (FWHM) and manifests very little energy dependence. Figure 7 shows the angular distribution of the events from the reaction $\nu_\mu + e^- \rightarrow \nu_\mu + e^-$.[1] The resolution of the forward peak again confirms the angular resolution of $\pm$ 5 mr. Its capability to identify $\nu_\mu e^-$ elastic scattering events from a background several thousand times larger proves the powerfulness of the detector.

During operation, each cathode delay-line signal was discriminated (at $\sim$300 μvolts) and both the leading and the trailing edge of the signal were timed with a resolution of 1 nsec. To help calibrate the system, each cathode amplifier had a test input to allow the injection of test signals onto the delay-line. Using these test signals, the amplifier gains and the transit times between tap points were precisely determined.

III. Acknowledgement

We wish to thank Professor Boyce McDaniel, Dr. R. Humphrey, and the staff members of the Wilson Synchrotom Laboratory at Cornell University for their enthusiastic and generous help in testing the detector. Professors S. C. Wright and R. M. Fine are acknowledged for their assistance. All the 49 chambers were constructed most skillfully by Kenneth Burns and John Dudas.

Reference

1. R. H. Heisterberg, L. W. Mo, T. A. Nunamaker; K. A. Lefler, A. Skuja; A. Abashian; N. E. Booth; C. C. Chang, C. Li, and C. H. Wang, to be published in Phys. Rev. Letters.

Figure Captions

Figure 1. Schematic of the detailed arrangement of the chamber.

Figure 2. Schematic showing the connection of anode wires to the G-10 strip.

Figure 3. (a) Test signal applied to the delay-line.

(b) Signal after traveling half the distance between two neighboring taps.

(c) Signal at the neighboring tap.

Figure 4. Experimental setup at Fermilab for measuring the reaction $\nu_\mu + e^- \rightarrow \nu_\mu + e^-$.

Figure 5. A typical angular resolution curve, obtained with 5 chambers and 4 GeV electrons.

Figure 6. Energy calibration of the chambers with electrons.

Figure 7. Angular distribution obtained in the experiment of measuring $\nu_\mu + e^- \rightarrow \nu_\mu + e^-$. Within the forward peak of 0 to 10 mr, there are 46 events.

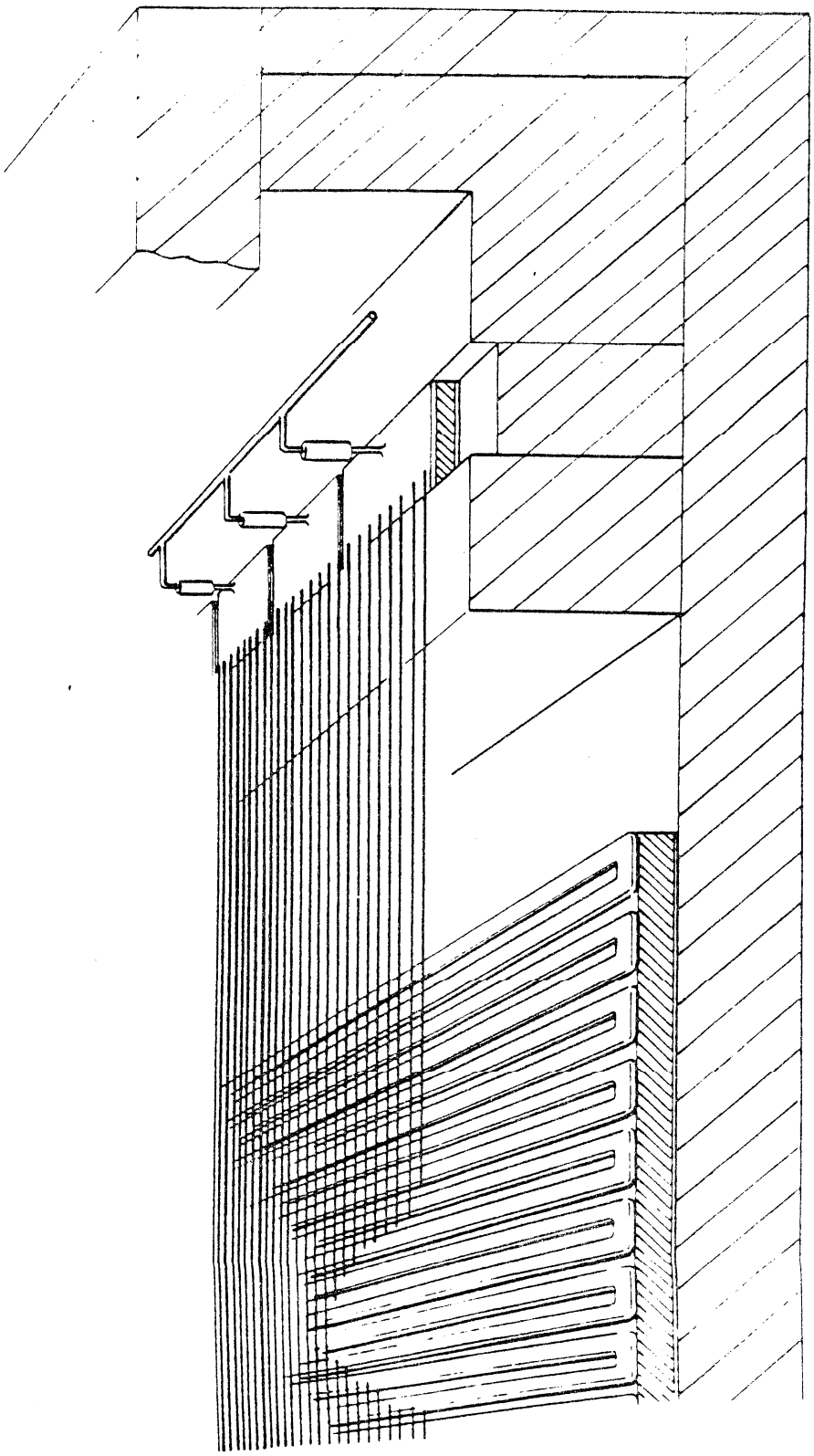

Fig. 1

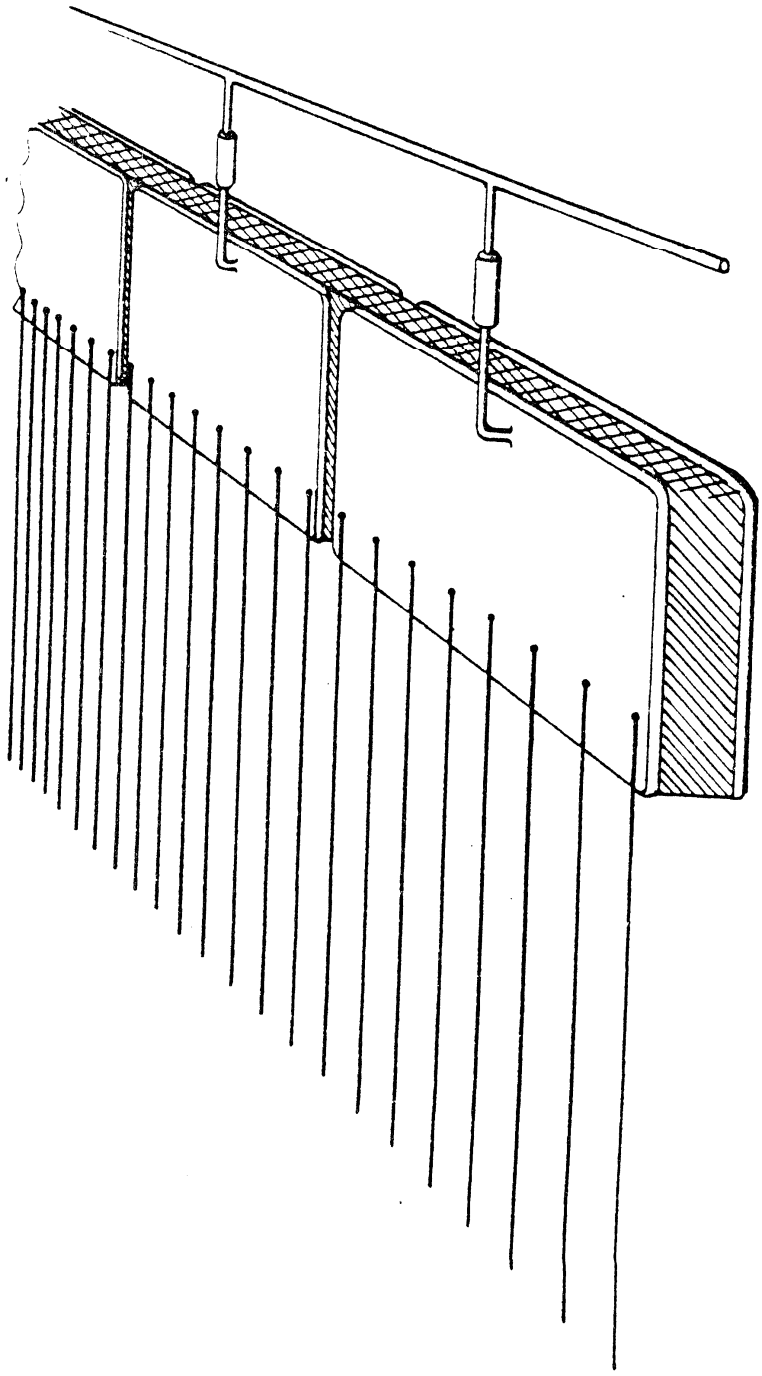

Fig. 2

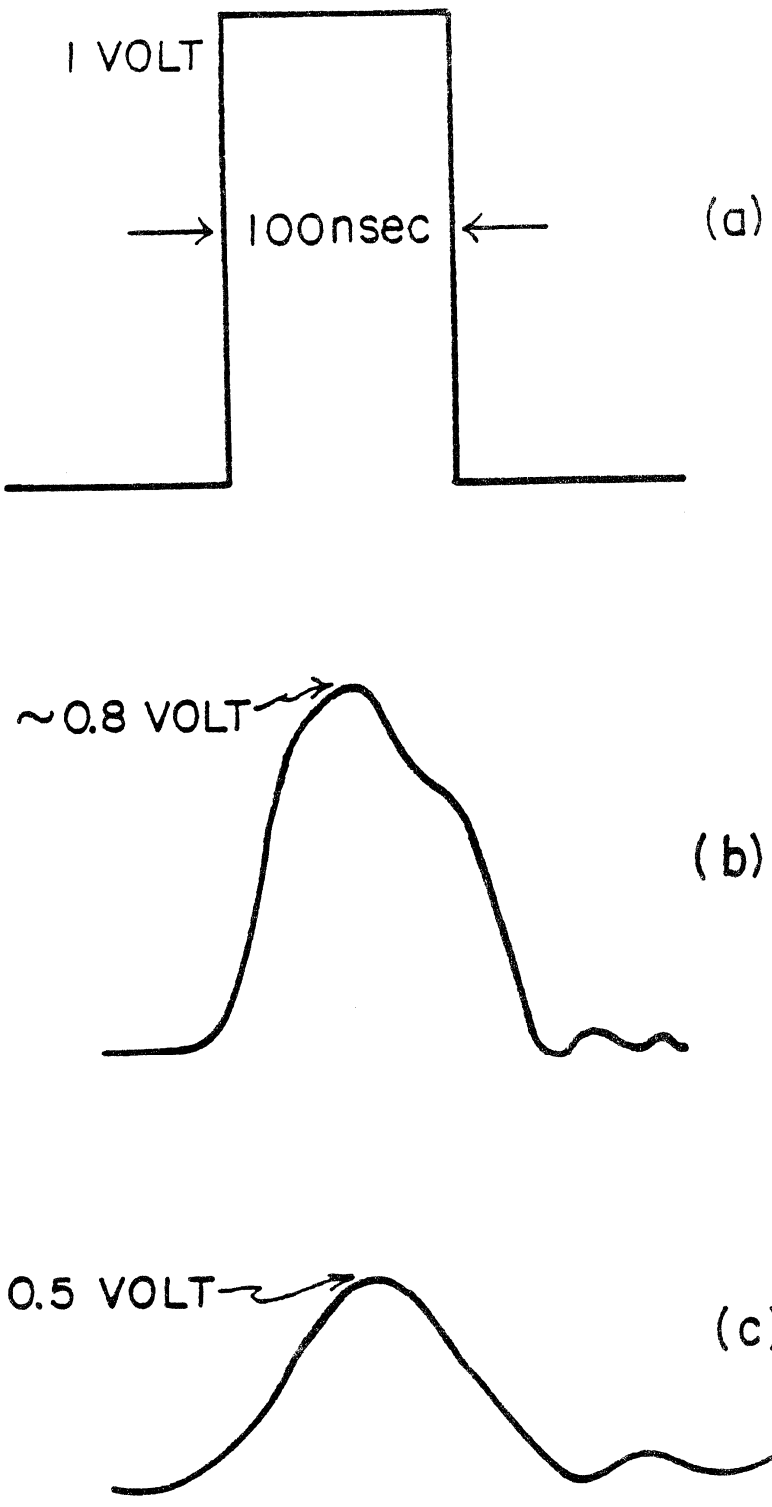

Fig. 3

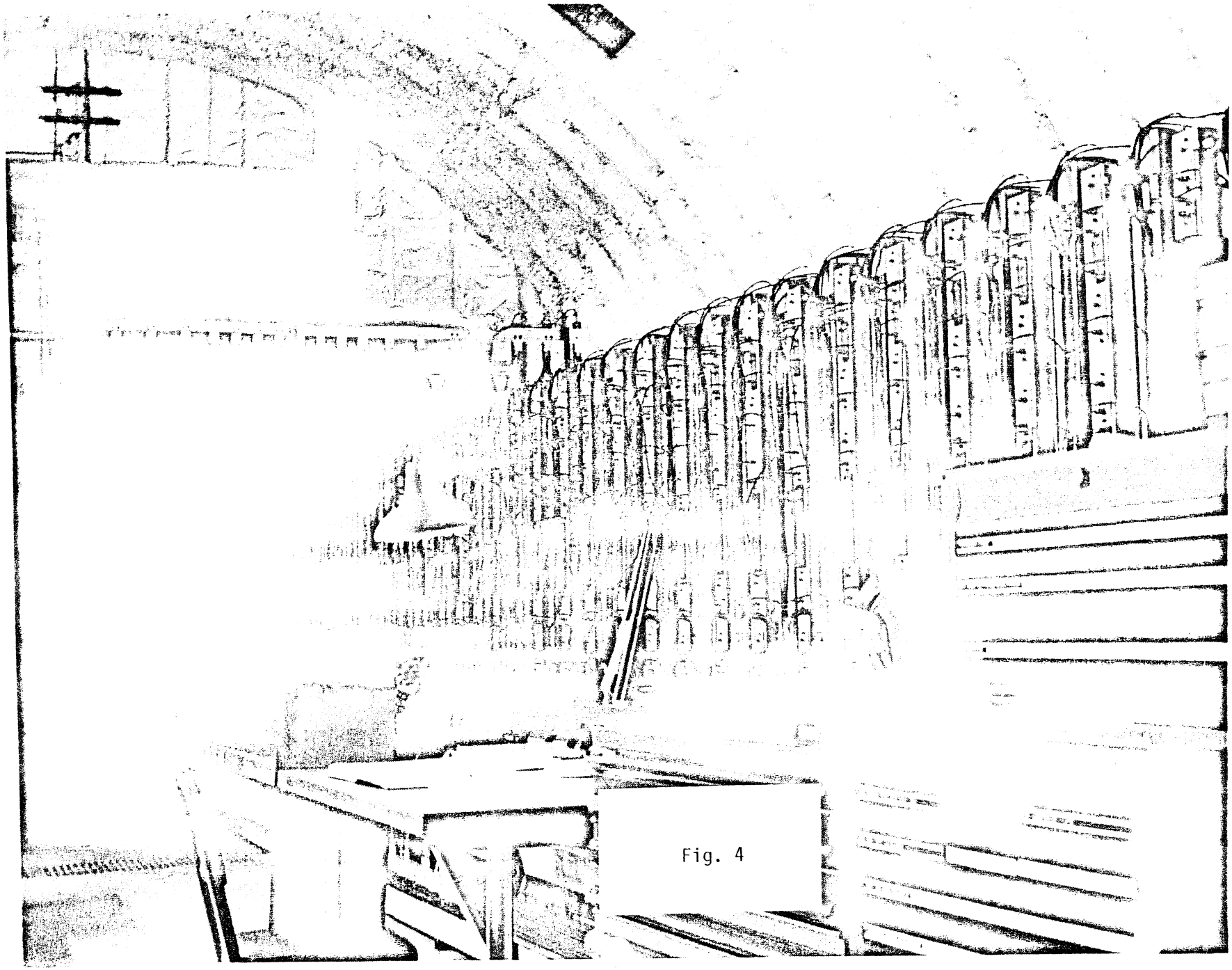

Fig. 4

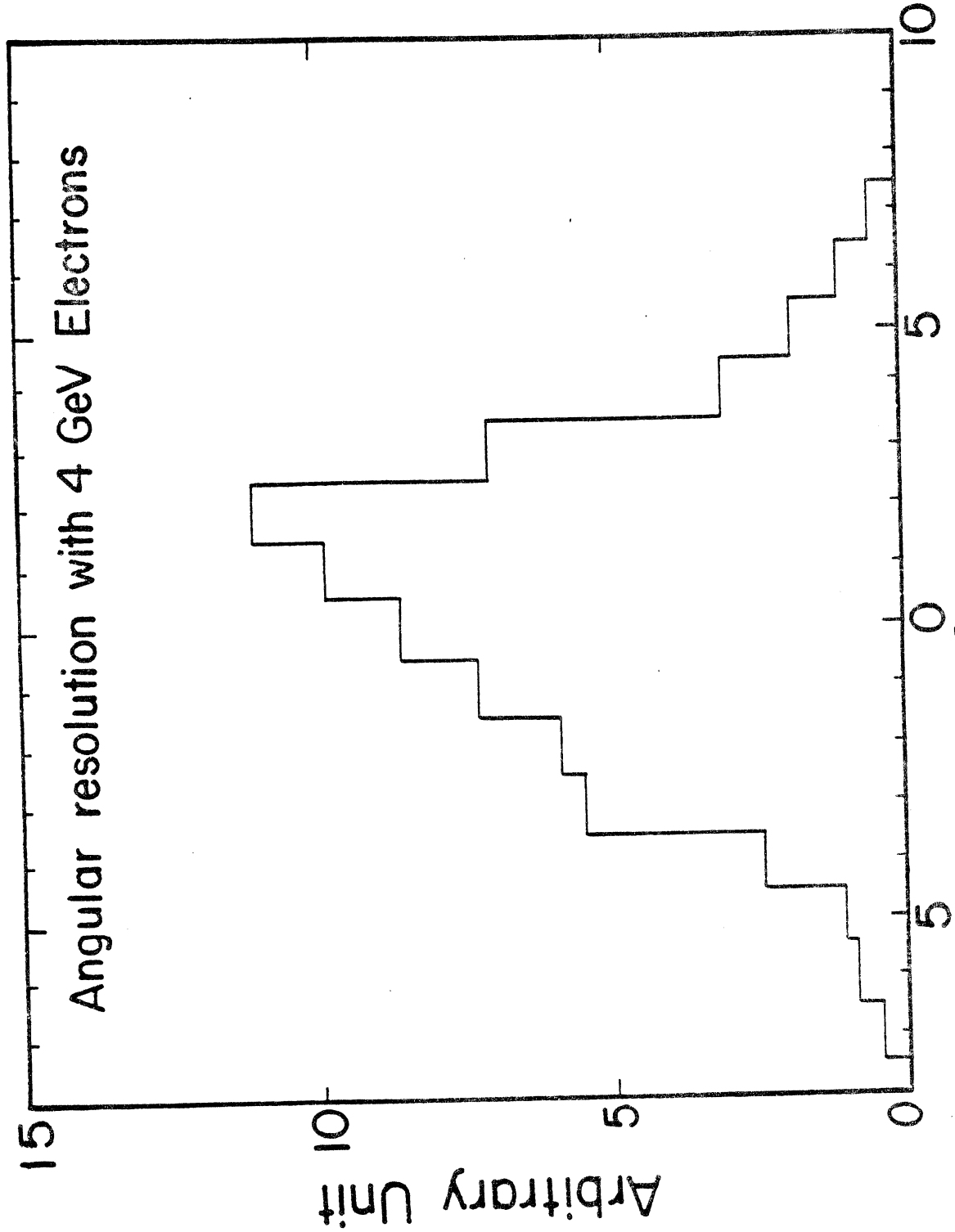
Angular resolution with 4 GeV Electrons
Arbitrary Unit
15
10
5
0
5
0
5
10
θ (mr)

Fig. 5

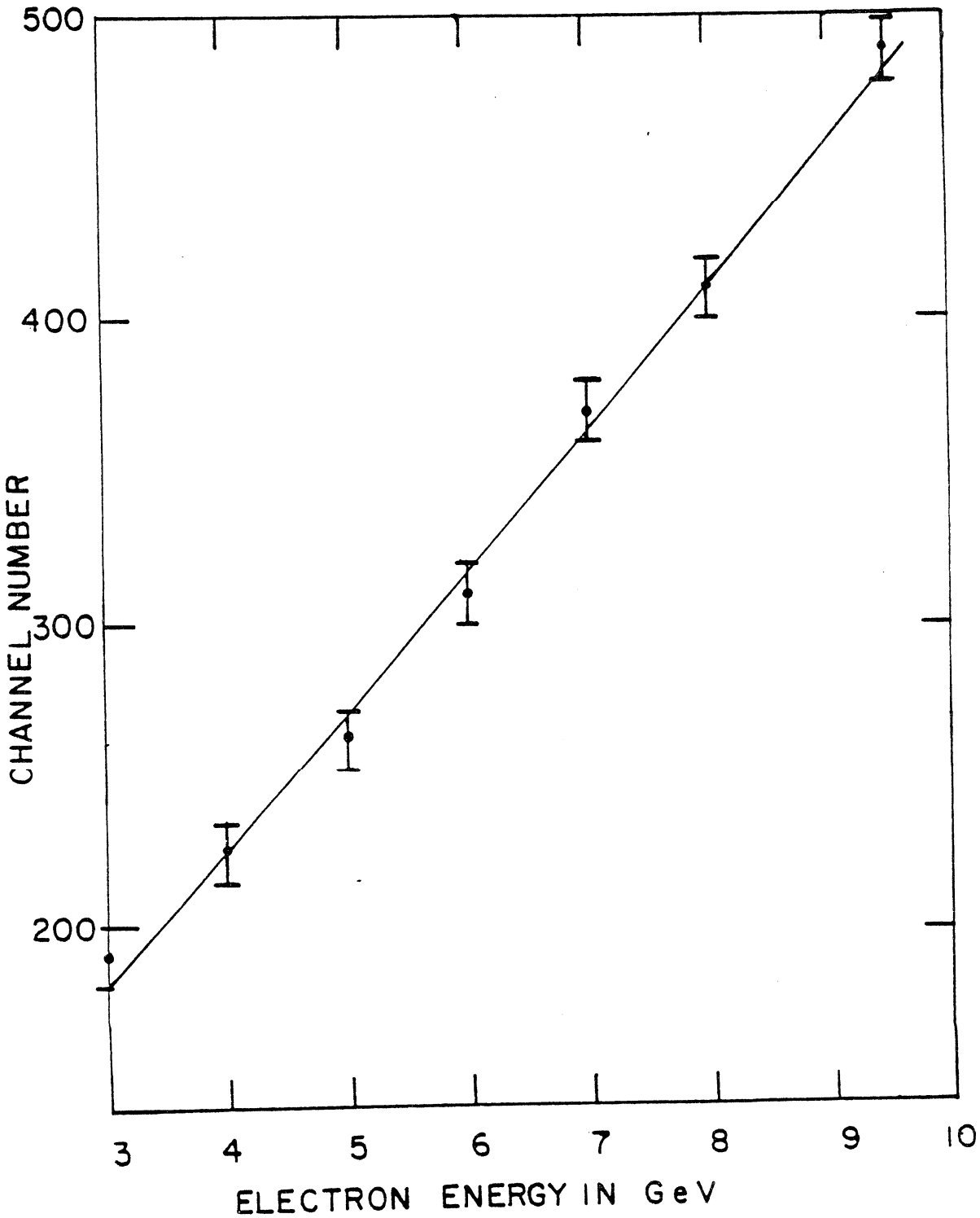
500
400
300
200
CHANNEL NUMBER
3
4
5
6
7
8
9
10
ELECTRON ENERGY IN GeV

Fig. 6

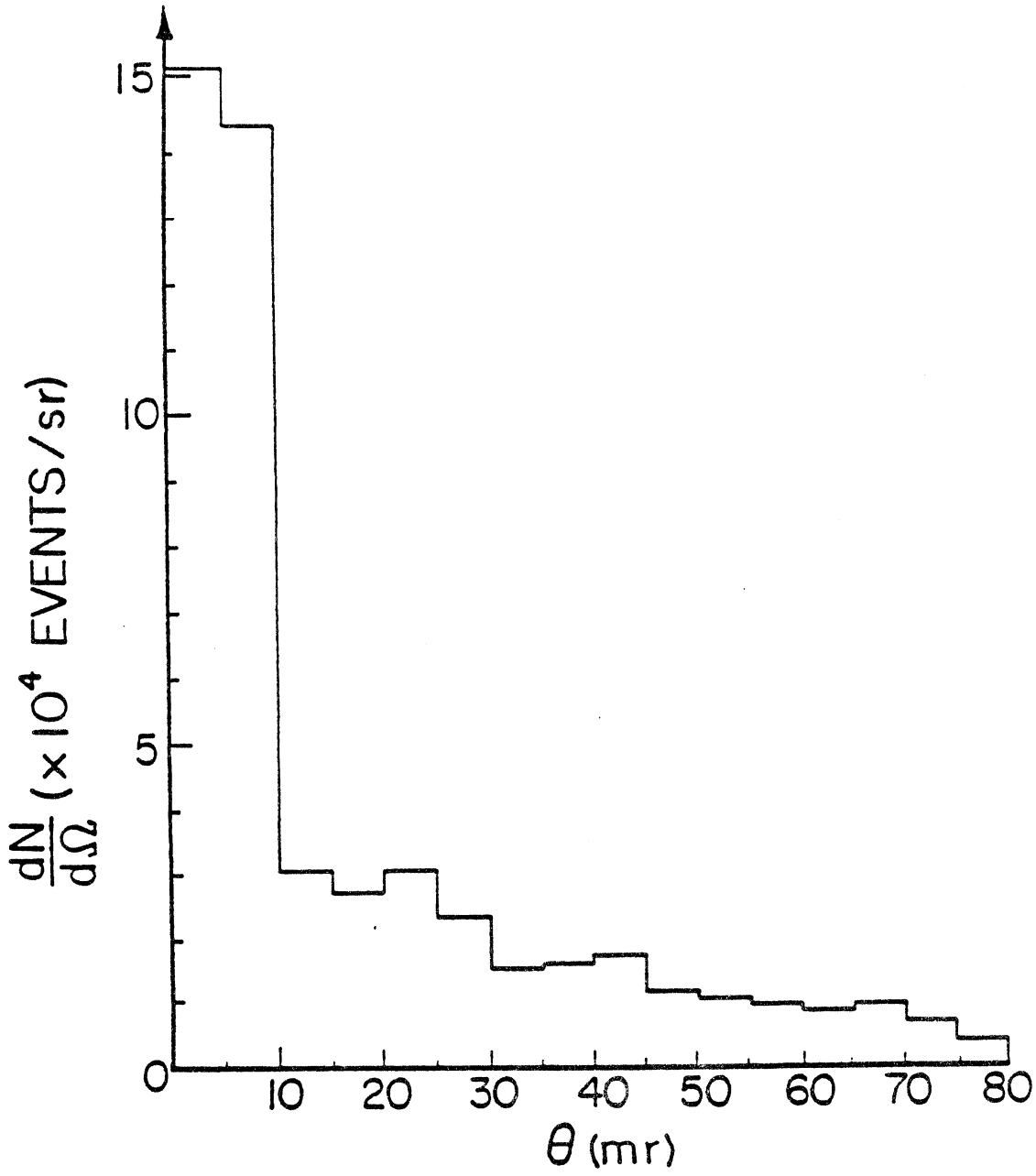

Fig. 7

Appendix 2

Equipment To Be Shipped To SLAC

The equipment to be shipped to SLAC for the Proposed Search experiment is listed below:

(1) 49 MWPC's, 42" x 42" in size, together with amplifiers and TDC's.

(2) 49 aluminum plates, 42" x 42" x 8 cm each . They belong to Fermilab and we have to arrange for their borrowing.

(3) 100 plastic scintillation counters for the calorimeter.

(4) Three plastic scintillation hodoscopes for front veto and muon detection.

(5) On-line computer: An Eclipse computer made by Data General. It includes 160 k words memory, one tape drive, one 98 MBytes disk drive, one Versatec printer, two video terminals, and one teletype.

(6) Trigger Box: Homemade, for generating the master trigger from the calorimeter.

Appendix 3

Equipment Needed from HEEP

Quantity	Type-description and/or model number
4	Modules, LR-612, X10 Amplifier
18	Modules, LRS-620, 100 MHz discriminators
2	Modules, LRS-380A, multiplicity logic unit
5	Modules, LRS-2249, CAMAC ADC
5	Modules, LRS-2259, CAMAC ADC (peak-sensing)
8	Modules, LRS-2341, CAMAC latches
8	Modules, LRS-127, Dual 8-Fold Fan-In
8	Modules, LRS-128, Dual 8-Fold Fan-Out
12	Modules, LRS-365, Dual 4-Fold Logic Unit
100	Channels, CAMAC Blind Scalers (100 MHz)
24	Channels, NIM Visual Scalers (100 MHz)
7	CAMAC Crates with Controllers and Cables
12	NIM Bins
1	Oscilloscope
3	Gate Generators
2	Pulsers
1	Beam Console and monitor unit
150	Channels of H. V. distribution box
8	H. V. Power Supplies (3 KV, 20 - 40 mA)
6	Delay Boxes
50	Channels of Positive H. V. (3 KV for MWPC's)